

Ciliary Motility: Regulation of Axonemal Dynein Motors

Rasagnya Viswanadha,¹ Winfield S. Sale,¹ and Mary E. Porter²

¹Department of Cell Biology, Emory University School of Medicine, Atlanta, Georgia 30322

²Department of Genetics, Cell Biology and Development, University of Minnesota, Minneapolis, Minnesota 55455

Correspondence: porte001@umn.edu

SUMMARY

Ciliary motility is crucial for the development and health of many organisms. Motility depends on the coordinated activity of multiple dynein motors arranged in a precise pattern on the outer doublet microtubules. Although significant progress has been made in elucidating the composition and organization of the dyneins, a comprehensive understanding of dynein regulation is lacking. Here, we focus on two conserved signaling complexes located at the base of the radial spokes. These include the I1/*f* inner dynein arm associated with radial spoke 1 and the calmodulin- and spoke-associated complex and the nexin–dynein regulatory complex associated with radial spoke 2. Current research is focused on understanding how these two axonemal hubs coordinate and regulate the dynein motors and ciliary motility.

Outline

- 1 Introduction
 - 2 Axonemal structure and a sliding microtubule model for ciliary bending
 - 3 Regulation of axonemal bending by I1/*f* dynein and the MIA complex located near RS1
 - 4 The RS2 regulatory complex and downstream regulation
 - 5 Conclusion
- References

1 INTRODUCTION

Cilia and flagella are highly conserved organelles required for cell signaling and cell motility in many organisms. They are generally classified either as immotile (including primary and sensory cilia) or as motile structures and play essential roles in vertebrate development and function of organs in the adult. We focus here on the structure and mechanisms of motile cilia that, in humans, are essential for embryonic development, sperm motility, and movement of fluid in the airway, oviducts, and brain ventricles. Ciliary motility is driven by the coordinated activity of the dynein motors. However, researchers are only beginning to understand the mechanisms that coordinate and control the dyneins. Here, we consider recent advances in genetic, cell-biological, and structural studies of ciliary dyneins and associated structures in *Chlamydomonas*. These studies have revealed new insights into the detailed organization of, and the physical interactions among, the dyneins.

In addition, we emphasize the organization of the outer doublet microtubule “96-nm repeat” and discuss two regulatory hubs required for control of ciliary motility: (1) radial spoke 1 (RS1) and its association with an inner dynein arm (IDA) called I1 dynein located near the proximal end of the 96-nm repeat, and (2) radial spoke 2 (RS2) and associated calmodulin- and spoke-associated complex (CSC) and the nexin–dynein regulatory complex (N-DRC) located at the distal end of the 96-nm repeat. Together, these two hubs are thought to coordinate dynein activity and regulate the ciliary waveform and beat frequency. These complexes are also important for modification of motility in response to external and internal signals. Other important topics not discussed here, but covered elsewhere, include the structure and function of the central pair microtubules (Smith and Yang 2004; Lechtreck and Witman 2007; O’Toole et al. 2012; Carbajal-Gonzalez et al. 2013; Oda et al. 2014a, 2014b), and theoretical models for ciliary bending (Brokaw 1985, 2009; Lindemann and Lesich 2010).

2 AXONEMAL STRUCTURE AND A SLIDING MICROTUBULE MODEL FOR CILIARY BENDING

2.1 Axoneme Structure in Motile Cilia

Motile cilia typically contain a “9 + 2” axoneme comprising nine outer doublet microtubules and a central apparatus built on two central pair microtubules and their associated projections (Fig. 1). Advances in electron microscopy (EM) have been essential to our understanding of the structure of the axoneme and the mechanism of mo-

tility in cilia. Key technical advances include computational approaches and image averaging (Kamiya et al. 1991; Mastronarde et al. 1992; Porter et al. 1992), rapid-freeze, deep-etch rotary-shadow EM (Goodenough and Heuser 1982; Goodenough and Heuser 1985), and, most recently, cryo-electron tomography (cryo-ET) of axonemes and intact cilia (Nicastro et al. 2006; Bui et al. 2009; Nicastro 2009; Bui and Ishikawa 2013; Oda and Kikkawa 2013). In most motile cilia, the nine outer doublet microtubules are organized with a structural axis that is fixed relative to the bending plane. For example, the inset in Figure 1A illustrates the forward (green circle) and reverse (blue circle) bends of the two flagella seen in a typical forward-swimming *Chlamydomonas* cell. In the cross section of an axoneme from *Chlamydomonas*, the bending plane passes between doublet #1 and doublet #2 (Fig. 1; and see Hoops and Witman 1983). As discussed below, dyneins present on the doublets on opposite sides of the axonemal axis are thought to be responsible for generating the forward (green) and reverse (blue) bends.

In vitro reactivation studies have revealed that all components necessary for movement are physically built into the axoneme (Gibbons and Gibbons 1972). Thus, study of isolated axonemes can reveal many of the features required for regulation of motility. *Chlamydomonas* has been a particularly powerful model organism for discovery of conserved genes required for ciliary assembly and motility because of its tractable genetics, informative mutant phenotypes, and the ease of culture for biochemical and structural studies (Harris 2009; Dutcher 2014; Kamiya and Yagi 2014).

2.2 Outer Doublet Microtubule Organization and Heterogeneity of Inner Dynein Arms

The focus of this review is on the structures of the outer doublet microtubules required to control the dynein motors (Figs. 1 and 2). Outer doublet components are organized in an axonemal 96-nm repeat and include the radial spokes (RSs), outer and IDAs, the CSC, and the N-DRC (Fig. 2). The outer dynein arms repeat once every 24 nm (Fig. 2) and are relatively homogeneous in structure (King and Kamiya 2009; King 2012; Kikkawa 2013; Kamiya and Yagi 2014; Owa et al. 2014). The subunit composition of the outer dynein arms in *Chlamydomonas* and humans is listed in Table 1 (Hom et al. 2011). The outer dynein arms are responsible for control of beat frequency and provide much of the power required for movement (Gibbons and Gibbons 1973; Kamiya and Okamoto 1985; Mitchell and Rosenbaum 1985; King and Kamiya 2009; Kamiya and Yagi 2014). Phenotypic analyses of outer dynein arm mutants have revealed that the dynein heavy chain (DHC) subunits



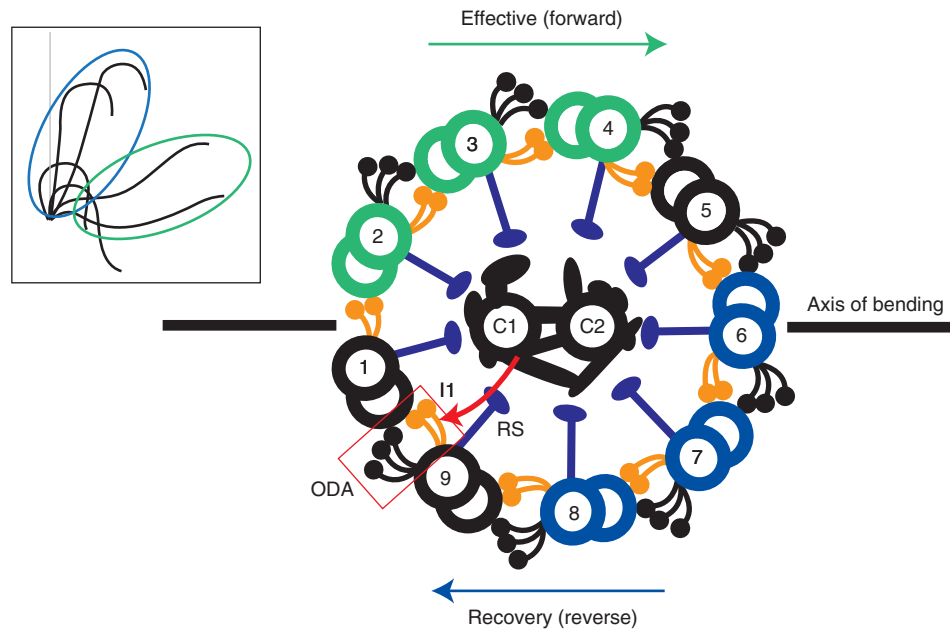


Figure 1. Cross section of the axoneme and illustration of the “switching model” for alternating forward and reverse bends. The 9 + 2 structure comprises nine outer doublet microtubules and a pair of singlet microtubules, C1 and C2, collectively known as the central pair. The outer doublet anchors the outer dynein arms (ODA), the radial spokes (RS), and the inner dynein arms, including I1 dynein. The black line passing through doublet #6 and between doublets #1 and #2 represents the plane/axis of bending. According to the switching model, when dyneins on one side of the axis are active (i.e., on doublets #2, #3, and #4), microtubule sliding can result in the forward, or effective, bend (green in *inset*). When the direction of bending reverses, the dyneins on doublets #2, #3, and #4 are inactivated, and dyneins on doublets #6, #7, and #8 are switched on to generate the recovery, or reverse, bend (blue in *inset*). (Adapted, with permission, from Smith 2007, © Journal of Cell Biology.)

α , β , and γ play distinct roles in regulation of flagellar motility. For example, the γ DHC interacts with the light chains LC1 and LC4 (King and Patel-King 2012; Ichikawa et al. 2014). The γ DHC–LC1–LC4 complex is thought to be important for part of the Ca^{2+} response and for feedback control in response to microtubule curvature (Morita and Shingyoji 2004; Hayashi and Shingyoji 2008; King 2010; King 2013). Additional models for the roles of the outer and IDAs and other functional domains in the outer dynein arms have been reviewed elsewhere (King and Kamiya 2009; Kamiya and Yagi 2014).

Based on analysis of wild-type and mutant *Chlamydomonas* cells, the IDAs are much more complex and contain at least 12 different DHC species (Porter et al. 1996; Yagi et al. 2009). The DHCs are organized into seven different major dyneins (labeled *a*, *b*, *c*, *d*, *e*, *f*/I1, and *g*) and at least three minor dyneins (DHC3, DHC4, and DHC11) that are distinct in composition (Table 2) and location in the 96-nm repeat (Fig. 2) (King and Kamiya 2009; Yagi et al. 2009; Bui et al. 2012; Heuser et al. 2012a; Kamiya and Yagi 2014). The IDAs are responsible for control of the size and shape of the forward and reverse ciliary bends.

2.3 A Sliding Microtubule/Switching Model for Ciliary Bending

Both structural and functional evidence supports a sliding microtubule model of ciliary bending. This evidence includes EM of cilia in defined bend positions (Satir 1968), observations by dark-field microscopy of dynein-driven microtubule sliding in protease-treated axonemes (Summers and Gibbons 1971), and direct demonstration that microtubule sliding occurs during axonemal bending (Shingyoji et al. 1977; Brokaw 1989).

Diverse data also support a switching model for alternating the pattern of forward and reverse bends (Satir and Matsuoka 1989; Smith 2007). The basis for this model stems from the discovery that axonemal dyneins are minus end–directed motors—that is, when active, dynein and its associated A tubule move in the proximal direction relative to the B tubule of the adjacent doublet (Sale and Satir 1977). Therefore, for ciliary bending to occur, the dyneins on all doublets cannot be active at the same time. Rather, there must be a switching mechanism that controls the activity of the dynein motors on different doublets and

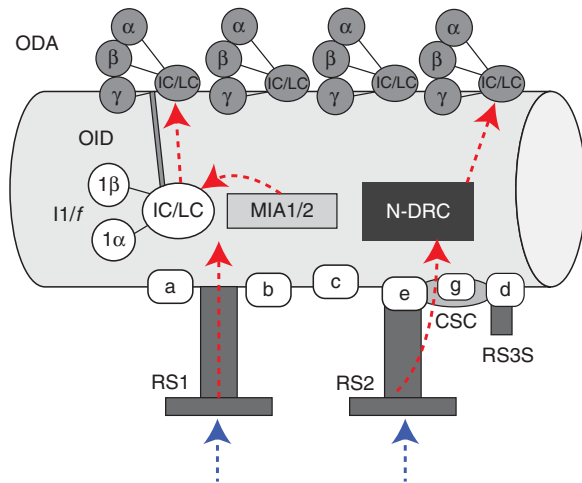


Figure 2. Parallel control pathways associated with the two regulatory hubs present in the 96-nm repeat: (1) RS1 and I1 dynein–MIA complex, and (2) RS2, CSC, and N-DRC. The blue arrows indicate chemical and mechanical signals that emanate from the central pair (CP) projections and are transmitted through the radial spoke heads to the bases of RS1 and RS2. The red arrows indicate signals transmitted from RS1 to the I1 dynein–MIA complex and from RS2 to the CSC and N-DRC, respectively, to control ciliary motility. The outer dynein arms (ODA) are also connected to both the I1–MIA complex and the N-DRC, also shown by the red arrows. CSC, calmodulin- and spoke-associated complex; N-DRC, nexin–dynein regulatory complex; IC, intermediate chain; LC, light chain; MIA, modifier of inner arms; RS, radial spoke. (Adapted from Yamamoto et al. 2013; King 2013.)

on opposite sides of the axis of bending (Fig. 1). Thus, the dyneins on one side of the axis of the axoneme are responsible for generating the forward bend, and the dyneins on the other side of the axis of the axoneme must produce the reverse bend. The most dramatic evidence for switching in the axoneme comes from the Shingyoji laboratory in which the investigators were able to activate dynein-driven sliding by physically bending doublet microtubules in isolated axonemes (Morita and Shingyoji 2004). Shingyoji and collaborators further determined that bending the doublet microtubules in the opposite direction activated microtubule sliding in the reverse direction (Hayashi and Shingyoji 2008). These results are consistent with regulation of dyneins by bending or structural distortion of the axoneme (Brokaw 1985; Lindemann and Mitchell 2007) and a switching model for alternating bend directions.

Further tests of the models will require a clear definition of active and nonactive states of the dynein motors. In the original studies by Goodenough and Heuser, the outer arms were observed in two different conformations, depending on the presence or absence of ATP (Goodenough and Heuser 1982). Recent cryo-ET analysis has also revealed distinct structures for the outer dynein arms in the presence or absence of ADP-vanadate (Movassagh et al. 2010). In

addition, cryo-ET of live sea urchin sperm flagella captured during movement by rapid freezing has revealed distinct structural conformations of the outer dynein arms on different outer doublet microtubules (see Supplemental Fig. 1 in Lin et al. 2014a).

Other key regulatory components of the 96-nm repeat include the two (or three) RSs and their associated substructures. Each RS is part of a distinct signaling hub: (a) RS1 is associated with IDAs 1 (I1 dynein or dynein f) and the MIA (modifier of inner arms) complex (King and Dutcher 1997; Wirschell et al. 2007; Yamamoto et al. 2013; Lin et al. 2014b), and (b) RS2 is associated with the CSC and N-DRC (Dymek et al. 2011; Heuser et al. 2012b; Porter 2012). Each hub is discussed in detail in Sections 3 and 4 below.

2.4 RS Heterogeneity

Common to both regulatory hubs are the RSs that are crucial for the regulation of dynein-driven motility as mutations that disrupt the assembly of the RSs typically result in complete flagellar paralysis (Witman et al. 1978). In vitro assays using isolated axonemes from wild-type and RS mutants further showed that the RSs increase microtubule sliding velocities, presumably through control of the dyneins (Smith and Sale 1992a). In most species, the RSs repeat as a set of triplets (RS1, RS2, RS3) every 96 nm along the length of the A tubule (Lin et al. 2014b). However, in a few organisms such as *Chlamydomonas*, the RSs repeat as pairs, RS1 and RS2, and a smaller structure, the RS stump or stand-in (RS3S), marks the position normally occupied by RS3 (Fig. 2) (Pigino et al. 2011; Barber et al. 2012; Lin et al. 2012). Biochemical studies have revealed that the RSs are large complexes comprising at least 23 different subunits (RSPs) that include a diverse group of structural and signaling proteins (Table 3) (Yang et al. 2006). These subunits have been assigned to specific regions of the RSs (e.g., head, neck, stalk, and base) by the analysis of different mutants and cryo-ET (Oda et al. 2014b).

In all species examined thus far, the detailed substructures of RS1 and RS2 are very similar, but RS2 contains two additional densities at its base, where it attaches to the A tubule (Pigino et al. 2012). The specific proteins located in the two additional RS2 densities are still unknown, but they probably correspond to a small subset of the RSPs identified previously as components of the RS stalk in *Chlamydomonas* (see Table 3) (Yang et al. 2006). Given that this region is the site of contact between RS2 and both the CSC and the N-DRC, it is also likely that the unique proteins in the additional RS2 densities, such as FAP206 (Vasudevan et al. 2015), play a role in mediating interactions among the three complexes (see Sec. 3).

Table 1. Features of outer dynein arms (ODAs) and associated proteins

| ODA | Protein and aliases ^a | <i>Chlamydomonas</i> gene (original) | Mutant strains | <i>Chlamydomonas</i> gene (current) | Human gene | Properties | References |
|---------------------|----------------------------------|--------------------------------------|--|-------------------------------------|-----------------------------|--|--|
| Heavy chains | HC1 α | ODA11 | <i>oda11</i> | DHC13 | – | ATPase/microtubule motor | Kamiya 1988; Mitchell and Brown 1994, 1997 |
| | HC1 β | ODA4 | <i>oda4</i> | DHC14 | DNAH9, DNAH11, DNAH17 | ATPase/microtubule motor | Kamiya 1988; Mitchell and Brown 1994 |
| | HC1 γ | ODA2 | <i>pf28</i> | DHC15 | DNAH5, DNAH8 | ATPase/microtubule motor | Kamiya et al. 1988; Mitchell and Rosenbaum (1985); Wilkerson et al. 1994 |
| Intermediate chains | IC1, IC78, IC80 | ODA9 | <i>oda9-1</i> , <i>oda9-2</i> (V5), <i>oda9-3</i> (V8), <i>oda9-4</i> (V24), <i>oda9-5</i> (V27) | DIC1 | DNAI1 | WD-repeat protein, binds α -tubulin, associates with multiple LCs | Kamiya 1988; Wilkerson et al. 1995 |
| | IC2, IC69, IC70 | ODA6 | <i>oda6-1</i> , <i>oda6-2</i> | DIC2 | DNAI2 | WD-repeat and coiled-coil protein, associates with multiple ICs | Kamiya 1988; Mitchell and Kang 1991 |
| Light chains | LC1 | – | – | DLU1 | DNAL1 | Leucine-rich repeat, binds γ HC motor domain | Patel-King and King 1995 |
| | LC2 | ODA12 | <i>oda12-1</i> , ^c <i>oda12-2</i> | DLT2 | TCTE3 | Homolog of Tctex2, required for outer-arm assembly | Pazour et al. 1999 |
| | LC3 | – | – | DLX1 | – | Thioredoxin, associates with β and γ HCs and LC7b | Dibella et al. 2004a; Wakabayashi and King 2006 |
| | LC4 | – | – | DLE1 | – | Ca ²⁺ binding, γ HC associated | Sakato et al. 2007 |
| | LC5 | – | – | DLX2 | – | Thioredoxin, associates with α HCs | Wakabayashi and King 2006 |
| | LC6 | ODA13 | <i>oda13</i> | DLL2 | – | LC8 homolog, dimer interacts with ICs and LC2 | King and Patel-King 2005 |
| | LC7a LC7b | ODA15 | <i>oda15</i> | DLR1 DLR2 | DYNLRB1 DYNLRB2 | Roadblock homolog, interacts with ICs Roadblock homolog, interacts with DC2 and LC3 | Dibella et al. 2004a Dibella et al. 2004a |
| | LC8 | FLA14 | <i>fla14-1,2,3</i> | DLL1 | DYNLL1 | Highly conserved, dimer interacts with ICs, also present in inner-arm I1/f and radial spokes, retrograde IFT motor | King and Patel-King 1995, Pazour et al. 1998 |
| | LC9 (Tctex1-like) | – | – | DLT1 | DYNLT1 | Tctex1 homolog, dimeric, interacts with IC1 and IC2 | Dibella et al. 2005 |
| | LC10, MOT24 | ODA12 | <i>oda12-1</i> ^b | DLL3 | DNAL4 | Tctex2, interacts with ICs and LC6 LC8 homolog, dimeric | Patel-King et al. 1997 |

Continued

Table 1. Continued

| ODA | Protein and aliases ^a | <i>Chlamydomonas</i> gene (original) | Mutant strains | <i>Chlamydomonas</i> gene (current) | Human gene | Properties | References |
|------------------|----------------------------------|--------------------------------------|--|-------------------------------------|--|---|--|
| Docking complex | DC1 | <i>ODA3</i> | <i>oda3-1</i> → <i>oda3-5</i> | <i>DCC1</i> | – | Docking complex, coiled-coil protein | Kamiya 1988; Takada and Kamiya 1994; Koutoulis et al. 1997 |
| | DC2 | <i>ODAI</i> | <i>oda1</i> | <i>DCC2</i> | <i>CCDC114</i> | Docking complex, coiled-coil protein | Kamiya 1988; Takada and Kamiya 1994; Takada et al. 2002 |
| | DC3 | <i>ODAI4</i> | <i>oda14-1</i> (V06), <i>oda14-2</i> (V16), <i>oda14-3</i> (F28), <i>oda14-11</i> | <i>DLE3</i> | – | Docking complex, binds Ca ²⁺ in a redox-sensitive manner | Koutoulis et al. 1997; Pazour et al. 1999, Casey et al. 2003 |
| Assembly factors | DCC3 | <i>ODA5</i> | <i>oda5-1</i> , <i>oda5-2</i> | <i>DCC3</i> | <i>CCDC63</i> | Coiled-coil protein, required for outer-arm assembly | Wirschell et al. 2004 |
| | ODA7 | <i>ODA7</i> | <i>oda7</i> | <i>DAU1</i> | <i>DNAAF1</i> (<i>LRRRC50</i>) | Leucine-rich repeats, purifies with the outer arm in the absence of I1/f; Putative ODA-I1 linker, required for the assembly of outer arms | Freshour et al. 2007 |
| | ODA8 | <i>ODA8</i> | <i>oda8</i> | <i>DLU2</i> | <i>LRRRC56</i> | Leucine-rich repeat protein, required for outer-arm assembly | Kamiya 1988; Kamiya 1995 |
| | ODA10 | <i>ODAI0</i> | <i>oda10</i> | – | – | Coiled-coil protein, required for outer-arm assembly | Kamiya 1988; Dean and Mitchell 2013 |
| | ODA16 | <i>ODA16</i> | <i>oda16</i> | <i>DAW1</i> | <i>WDR69</i> | WD-repeat, required for outer-arm transport to the cilium | Ahmed and Mitchell 2005 |
| | PF13 | <i>PF13</i> | <i>pf13-1</i> → <i>pf13-3</i> | <i>DAPI</i> | <i>DNAAF2</i> | PIH domain containing, required for preassembly of outer arms and a subset of inner arms | Omran et al. 2008 |
| | PF22 | <i>PF22</i> | <i>pf22</i> , <i>pf22A</i> | <i>DABI</i> | <i>DNAAF3</i> | Required for outer-arm assembly | Huang et al. 1979; Mitchison et al. 2012 |
| | – | – | – | – | <i>TXNDC3</i> (<i>Sptrx2</i>) ^c | Thioredoxin-nucleoside diphosphate kinase, partial lack of ODA | Dureiz et al. 2007 |

HC, Heavy chain; IC, intermediate chain; LC1–LC9, light chains; DC, docking complex; WD, tryptophan–aspartic acid; IFT, intraflagellar transport; PIH, protein interacting with HSP90.

^aThe current preferred protein name is indicated first in bold type.

^bThe *DIT2* and *DLL3* genes are adjacent; both are completely deleted in *oda12-1*.

^cHuman patients possessing a mutation in this gene show a wide range of ciliopathies, including primary ciliary dyskinesia (PCD).

Table 2. Inner dynein arms (IDAs) and associated proteins

| IDA | Protein aliases ^a | <i>Chlamydomonas</i> gene (original) | <i>Chlamydomonas</i> gene (current) | Human gene | Mutant strains | Properties | References |
|----------------------------------|------------------------------|--------------------------------------|-------------------------------------|-------------------|---|---|--|
| II/ <i>f</i> heavy chains | HC1 α | IDA1 | DHC1 | DNAH10 | <i>ida1-1</i> \rightarrow <i>ida1-6/pf9-1</i> \rightarrow <i>pf9-4/pf30</i> | ATPase/microtubule motor | Kamiya et al. 1991; Piperno et al. 1990; Myster et al. 1997; Myster et al. 1999; Porter et al. 1992 |
| | HC1 β | IDA2 | DHC10 | DNAH2 | <i>ida2-1</i> \rightarrow <i>ida2-6</i> | ATPase/microtubule motor | Kamiya et al. 1991; Perrone et al. 2000 |
| | IC140 | IDA7 | DIC3 | WDR63 | <i>ida7</i> | WD-repeat protein, associates with tubulin and other ICs | Perrone et al. 1998; Yang and Sale 1998 |
| II/ <i>f</i> intermediate chains | IC138 | BOP5 | DIC4 | WDR78 | <i>bop5-1</i> \rightarrow <i>bop5-6</i> | WD-repeat protein involved in phosphorylation-based regulation; forms a complex with IC97, FAP120, and LC7b | King and Dutcher 1997; Hendrickson et al. 2004; Bower et al. 2009; Ikeda et al. 2009; VanderWaal et al. 2011 |
| | IC97, IC110 | - | DII6 | LAS1 ^b | - | Interacts with IC140, IC138, and tubulin | Wirschell et al. 2009 |
| II/ <i>f</i> light chains | FAP120 ^c | - | DII7 | - | - | Present in the IC138 subcomplex | Ikeda et al. 2009 |
| | Tctex1 | - | DIT3 | DYNLT3 | - | Dimeric, LC9 homolog | Harrison et al. 1998; Dibella et al. 2001; Dibella et al. 2004a |
| | Tctex2b | - | DIT4 | TCTEX1D2 | <i>pf16(D2)</i> ^d | LC2 homolog | Dibella et al. 2004b |
| | LC7a, LC7 | ODA15 | DLR1 | DYNLRB1 | <i>oda15</i> | Shared with outer-arm dynein | Dibella et al. 2004a |
| II/ <i>f</i> associated proteins | LC7b | - | DLR2 | DYNLRB2 | - | Shared with outer-arm dynein and interacts with IC138 | Dibella et al. 2004a |
| | LC8 | FLA14 | DLL1 | DYNLL1, DYNLL2 | <i>fla14-1, fla14-2</i> | Shared with outer-arm dynein, dimeric | Wirschell et al. 2009 |
| | FAP73 | MIA1 | MIA1 | - | <i>mia1</i> | Associates with FAP100 in the MIA complex and with IC138 | King and Dutcher 1997; Yamamoto et al. 2013 |
| | FAP100 | MIA2 | MIA2 | - | <i>mia2</i> | Associates with FAP73 in the MIA complex and with IC138 | King and Dutcher 1997; Yamamoto et al. 2013 |
| Monomeric IDA heavy chains | DHC6 | DHC6 | DHC6 | DNAH12 | - | ATPase/microtubule motor, monomeric | Porter et al. 1996; Yagi et al. 2009 |
| | DHC5 | DHC5 | DHC5 | DNAH7 | - | ATPase/microtubule motor, monomeric | Porter et al. 1996; Bui et al. 2012 |
| | DHC9 | IDA9 | DHC9 | - | <i>ida9</i> | ATPase/microtubule motor, monomeric | Porter et al. 1996; Yagi et al. 2005 |
| | DHC2 | DHC2 | DHC2 | DNAH1, 6 | - | ATPase/microtubule motor, monomeric | Porter et al. 1996; Bui et al. 2012 |
| | DHC8 | DHC8 | DHC8 | DNAH14 | - | ATPase/microtubule motor, monomeric | Porter et al. 1996; Yagi et al. 2009 |
| | DHC7 | DHC7 | DHC7 | - | - | ATPase/microtubule motor, monomeric | Porter et al. 1996; Yagi et al. 2009 |
| | - | - | - | - | - | species <i>g</i> | - |

Continued

Table 2. Continued

| IDA | Protein and aliases ^a | <i>Chlamydomonas</i> gene (original) | <i>Chlamydomonas</i> gene (current) | Mutant strains | Human gene | Properties | References |
|--------------------------------|----------------------------------|--------------------------------------|--|----------------|--|--|---|
| DHC4 | DHC4 | DHC4 | DHC4 | – | <i>DNAH3</i> | ATPase/microtubule motor, minor monomeric species | Porter et al. 1996; Yagi et al. 2009 |
| DHC11 | DHC11 | DHC11 | DHC11 | – | – | ATPase/microtubule motor, minor monomeric species | Porter et al. 1999; Yagi et al. 2009 |
| DHC3 | DHC3 | DHC3 | DHC3 | – | – | ATPase/microtubule motor, minor monomeric species | Porter et al. 1996; Yagi et al. 2009 |
| Actin | IDA5 | <i>IDA5</i> (<i>ACT1</i>) | <i>ida5</i> | – | <i>Actin</i> ^e | Essential for the assembly of species <i>a</i> , <i>c</i> , <i>f</i> , <i>e</i> , and one minor dynein | Kato-Minoura 1997 |
| NAP1 associated proteins | NAP1 | <i>NAP1</i> (<i>ARPI2</i>) | – | – | – | Novel actin-related protein that can functionally replace actin for species <i>b</i> and <i>g</i> assembly | Hirono et al. 2003 |
| p28 | IDA4 | <i>DIII</i> | <i>ida4-1</i> → <i>ida4-3</i> | – | <i>DNALI1</i> | Essential for assembly of species <i>a</i> , <i>c</i> , and <i>d</i> ; dimeric and binds amino-terminal region of HC | Kamiya et al. 1991; LeDizet and Piperno 1995 |
| Centrin | VFL2 | <i>DLE2</i> (<i>CNT1</i>) | <i>vfl2-1</i> , <i>vfl2-R1</i> , <i>vfl2-R5</i> , <i>vfl2-R8</i> , <i>vfl2-R10</i> , <i>vfl2-R11</i> , <i>vfl2-R13</i> | – | <i>CETN1</i> , <i>CETN2</i> , <i>CETN3</i> | Ca ²⁺ -binding protein, associates with amino-terminal portion of heavy chain and actin | Huang et al. 1988; Sanders and Salisbury 1989; Yanagisawa and Kamiya 2001 |
| p38 | – | <i>DII2</i> | – | – | <i>ZMYND12</i> | Associates with species <i>d</i> only | Yamamoto et al. 2006 |
| p44 | – | <i>DII3</i> | – | – | <i>TTC28</i> | Associates with species <i>d</i> only | Yamamoto et al. 2008 |
| Monomeric IDA assembly factors | MOT48 | <i>IDA10</i> | <i>ida10-1</i> | – | <i>PHI1D1</i> | PIH protein, required for the preassembly of a subset of inner arms | Yamamoto et al. 2010 |

HC, heavy chain; IC, intermediate chain; LC2, LC7, LC7a, LC7b, LC8, light chains; MIA, modifier of inner arms; PIH, protein interacting with HSP90.

^aThe current preferred protein name is indicated first in bold type.

^bRelated to vertebrate Las1.

^cEAP120 is listed here as an intermediate chain subunit.

^d*pfl6(D2)* lacks both the *DII4* and *PIF16* genes; the latter encodes a component of the central pair apparatus.

^eFor organisms that express multiple actin isoforms, it has not been determined which isoform(s) is present in the cilia/flagella.

Table 3. Radial spoke-associated proteins (RSPs) and calmodulin- and spoke-associated complex proteins (CaM-IPs)

| <i>Chlamydomonas</i> name | MW (kDa) | Motifs | Position | <i>Homo sapiens</i> name | References |
|----------------------------|----------|-----------------------------------|-----------|--------------------------|------------------------|
| RSP1 | 78.6 | MORN | Head | RSPH1 | Yang et al. 2006 |
| RSP2 | 77.4 | DPY, GAF, CaM binding | Neck | DYDC2 | Yang et al. 2006 |
| RSP3 | 56.8 | AKAP motif | Stalk | RSPH3 | Williams et al. 1989 |
| RSP4 | 49.8 | Unknown | Head | RSPH4A/6A | Curry et al. 1992 |
| RSP5 | 48.8 | Aldo-keto reductase | Stalk | – | Yang et al. 2006 |
| RSP6 | 48.8 | Unknown | Head | RSPH4A/6A | Curry et al. 1992 |
| RSP7 | 55 | RII a/EF hand | Stalk | CALML5 | Yang et al. 2006 |
| RSP8 | 40.5 | Armadillo | Stalk | ARMC4 | Yang et al. 2006 |
| RSP9 | 29.5 | Unknown | Head | RSPH9 | Yang et al. 2006 |
| RSP10 | 23.5 | MORN | Head | RSPH1/10B | Yang et al. 2006 |
| RSP11 | 21.5 | RII a | Stalk | ROPN1L | Yang et al. 2006 |
| RSP12 | 19.7 | Peptidyl-prolyl isomerase | Stalk | PPIL6 | Yang et al. 2006 |
| RSP13 | ~98 | Unknown | Stalk | – | Yang et al. 2006 |
| RSP14 | 28.3 | Armadillo | Stalk | RTDR1 | Yang et al. 2006 |
| RSP15 | ~38 | LRR | Stalk | – | Yang et al. 2006 |
| RSP16 | 39 | DnaJ/DnaJ-chaperone | Neck | DNAJB13 | Yang et al. 2006 |
| RSP17 | 98.5 | GAF | Stalk | – | Yang et al. 2006 |
| RSP18/CaM-IP2 ^a | 183 | AKAP/AAT-1, IQ | Stalk/CSC | C3orf15, MAATS1 | Dymek and Smith 2007 |
| RSP19/CaM-IP3 ^a | 140 | Pyridine-disulfide oxidoreductase | Stalk/CSC | C20orf26 | Dymek and Smith 2007 |
| RSP20 | 18.3 | EF hand (calmodulin) | Stalk/CSC | Calmodulin | Yang et al. 2001 |
| RSP21 | 16 | – | Stalk | – | Yang et al. 2006 |
| RSP22/LC8 | 10.3 | LC8 | Stalk | DYNLL2 | Yang et al. 2009 |
| RSP23 | 61 | NDK, DPY, IQ | Neck | NME5 | Patel-King et al. 2004 |
| CaM-IP4 ^a | 100 | WD repeat | Stalk/CSC | WDR66 | Dymek and Smith 2007 |

AKAP, A kinase anchoring protein motif; LRR, leucine-rich repeat; MORN, membrane occupation and recognition nexus; NDK, nucleoside diphosphate kinase motif; WD, WD40 repeat; DPY, Dpy-30 motif; GAF, cGMP, adenyl cyclase, FhIA domain; IQ, calmodulin-binding domain; CSC, calmodulin- and spoke-associated complex.

^aCaM-IP2, CaM-IP3, and CaM-IP4 are also known as FAP91, FAP61, and FAP251 (Dymek and Smith 2007).

3 REGULATION OF AXONEMAL BENDING BY I1/f DYNEIN AND THE MIA COMPLEX LOCATED NEAR RS1

3.1 I1/f Dynein Is a Conserved Two-Headed Inner Dynein Arm

The number and complexity of inner-arm dyneins have made it challenging to define their individual contributions to motility, but nearly all the inner-arm mutants characterized thus far display some defects in their flagellar waveform (Kamiya and Yagi 2014). In particular, several studies have shown that I1/f dynein is required for normal control of ciliary bending (Brokaw and Kamiya 1987; Bayly et al. 2010; VanderWaal et al. 2011). For example, *Chlamydomonas* mutants that fail to assemble I1 dynein show slow, smooth forward swimming, decreased dynein-driven microtubule sliding, abnormal ciliary waveforms and reduced phototaxis (reviewed in Wirschell et al. 2007; see also Porter and Sale 2000; Wirschell et al. 2007; Kamiya and Yagi 2014). However, the precise mechanism by which I1 dynein modulates ciliary bending remains unknown.

I1 dynein is the only inner-arm subspecies that contains two distinct DHCs. Each I1 DHC is highly conserved and

widely distributed among ciliated eukaryotes (Wickstead and Gull 2007). Additional unique features of I1 dynein suggest that I1 dynein and the MIA complex (King and Dutcher 1997; Yamamoto et al. 2013) play an important role in control of ciliary bending. We discuss models in which I1 dynein could operate through (a) a direct interaction with other axonemal dyneins to regulate their motor activity and (b) resisting microtubule sliding driven by other axonemal dyneins.

I1 dynein was first identified by analysis of slow swimming mutants (Piperno et al. 1990; Kamiya et al. 1991; Porter et al. 1992). It is located in the proximal end of each 96-nm repeat near RS1 (Figs. 1 and 2), and it makes contact with many other structures in the axoneme, including the ODA and neighboring single-headed IDAs (Heuser et al. 2012a). I1 dynein can be easily extracted from isolated axonemes and purified as an intact 20S complex (Piperno et al. 1990; Porter et al. 1992) comprising two heavy chains (1 α and 1 β), three intermediate chains (IC97, IC140, and IC138), and five light chains (Tctex1, Tctex2b, LC7a, LC7b, and LC8) (Fig. 3 inset; Tables 1 and 2). In addition, partial complexes of I1 dynein can assemble in the absence of IC138 and associated proteins defining a “IC138 sub-



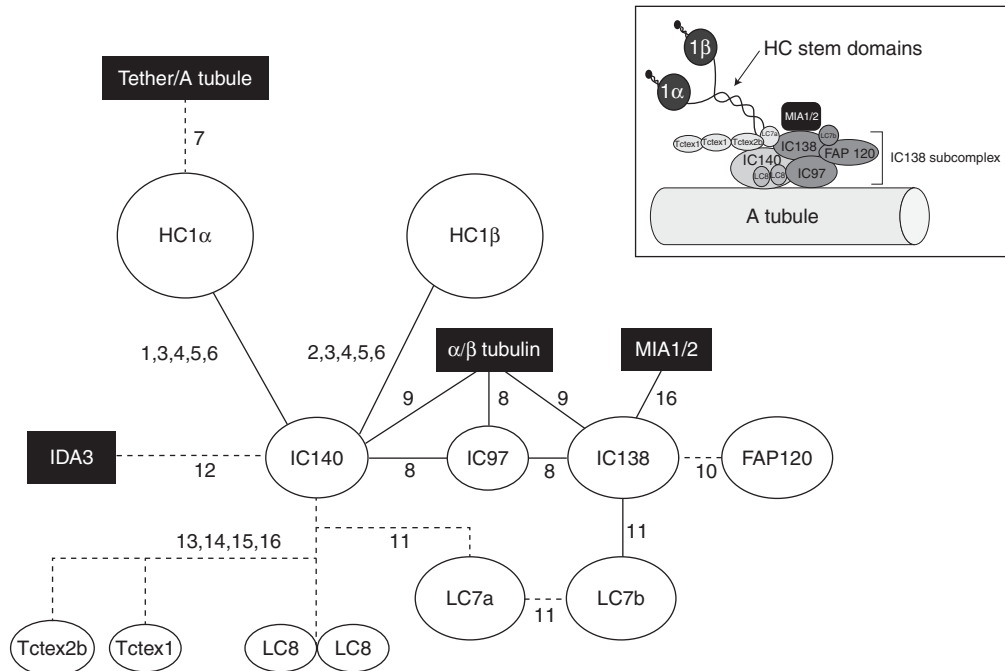


Figure 3. Diagram of interactions within I1 dynein and with the MIA complex and associated proteins. As illustrated in the *inset*, I1 dynein contains two distinct heavy chain motor domains (HC1 α and HC1 β), three intermediate chains (IC140, IC97, and IC138), and five light chains (Tctex1, Tctex2b, LC8, LC7a, and LC7b). The solid lines represent protein–protein interactions determined by biochemical and/or structural analysis of I1 dynein assembly mutants (1: Myster et al. 1997; 2: Perrone et al. 2000; 3: Bower et al. 2009; 4: Toba et al. 2011; 5: VanderWaal et al. 2011; 6: Perrone et al. 1998; 8: Wirschell et al. 2009; 9: Hendrickson et al. 2004; 11: DiBella et al. 2004a; 16: Yamamoto et al. 2013). The dashed lines indicate predicted interactions based on the analysis of I1 assembly mutants (6: Perrone et al. 1998; 7: Heuser et al. 2012a; 10: Ikeda et al. 2009; 11: DiBella et al. 2004a; 12: Viswanadha et al. 2014; 13: Wu et al. 2005; 14: Harrison et al. 1998; 15: Yang et al. 2009; 16: DiBella et al. 2004b). (Adapted from DiBella et al. 2004a; King 2013.)

complex” comprising IC138, IC97, FAP120, and LC7b (Fig. 2, inset) (Hendrickson et al. 2004; Bower et al. 2009; Wirschell et al. 2009). Analysis of IC138 (*bop5*) mutants has revealed that the IC138 subcomplex, like I1 dynein, is essential for control of ciliary waveform (Brokaw and Kamiya 1987; Bayly et al. 2010; VanderWaal et al. 2011).

3.2 The MIA Complex Interacts with I1 Dynein

I1 dynein has been shown to physically interact with the MIA complex that was discovered by genetic, biochemical, and structural analysis of *Chlamydomonas* mutants defective in light-regulated movement (phototaxis) (King and Dutcher 1997; Yamamoto et al. 2013). Cryo-ET analysis of wild-type and *mia* mutants revealed that the MIA complex is located near the IC138 complex between I1 and the N-DRC (Fig. 2) (Yamamoto et al. 2013). The complex comprises two coiled-coil protein subunits MIA1 and MIA2. Motility analysis of the mutants *mia1* and *mia2* revealed a slow swimming phenotype similar to that of mutants lacking I1 dynein. Further genetic and phenotypic analysis revealed that I1 dynein and the MIA complex might act as a

functional unit to control ciliary movement (Yamamoto et al. 2013).

3.3 Mutations Reveal Functional Domains in I1 Dynein

Several mutations in I1 subunits have been extremely useful in providing detailed information on the roles of individual subunits in the assembly of the I1 complex and/or function of the I1 dynein complex in ciliary motility (Bower et al. 2009; Wirschell et al. 2009; Toba et al. 2011; VanderWaal et al. 2011; Heuser et al. 2012a). For instance, most mutations in genes that encode 1 α and 1 β DHCs or the intermediate chain subunit IC140 result in a complete failure in I1 dynein assembly, leaving a gap in every 96-nm repeat (Piperno et al. 1990; Kamiya et al. 1991; Porter et al. 1992; Myster et al. 1997; Perrone et al. 1998; Myster et al. 1999; Perrone et al. 2000). Notably, loss of the I1 dynein does not affect the assembly of other IDAs, RSs, outer-arm dyneins, or the MIA complex, indicating that the targeting and assembly of I1 dynein is independent of other axonemal components (Piperno et al. 1990; Kamiya et al. 1991; Porter

et al. 1992; Smith and Sale 1992b; Bui et al. 2012; Heuser et al. 2012a; Yamamoto et al. 2013). Thus, interpretation of I1 mutant phenotypes (Brokaw and Kamiya 1987; Bayly et al. 2010; VanderWaal et al. 2011) is not complicated by failure of assembly of additional axonemal components.

Interestingly, however, both I1 DHC mutations can be partially rescued by transformation with DHC constructs lacking the dynein motor domains, indicating that the motor domains are not required for the assembly of the I1 complex (Myster et al. 1999; Perrone et al. 2000). The mutant strains lacking either the 1α or 1β motor domains assemble the remainder of I1 dynein at the correct location in the axoneme (Myster et al. 1999; Perrone et al. 2000). These studies pinpointed the location of both dynein-motor domains within the structure of the 96-nm repeat (Fig. 2). Toba and colleagues (Toba et al. 2011) took advantage of these mutants to show that each motor domain has distinct properties in *in vitro* microtubule sliding and translocation assays. The investigators proposed that one of the functions of I1 dynein is inhibition of microtubule sliding driven by other axonemal dyneins (Toba et al. 2011). Consistent with this model, Kotani and colleagues (Kotani et al. 2007) used *in vitro* microtubule translocation experiments to show that purified I1 dynein, when mixed with purified IDA *c*, impeded microtubule translocation driven by dynein *c*.

These data support a model in which I1 dynein acts as a brake to slow and locally regulate sliding driven by the outer dynein arm and other IDAs. Consistent with this model, studies of the double mutants lacking I1 dynein and the RSs or the central pair (both of which are required for dynein-driven sliding), display an increase in microtubule sliding velocities compared with RS or central pair mutants alone (Yang and Sale 2000; Smith 2002). One interpretation of this observation is that the increase in velocity of sliding in mutants lacking I1 dynein is due to the loss of resistance to microtubule sliding.

Thus, the I1 dynein appears to play two distinct roles—contributing to microtubule sliding on the one hand, but also resisting microtubule sliding by other dyneins. Cryo-ET later revealed that the two I1 motor domains differ with respect to their connections to other structures within the axoneme. The 1β motor domain is closer to the IC–LC complex and the outer dynein arms, whereas the 1α motor domain is closer to its neighboring inner-arm dynein and is also tethered to the underlying A tubule (Heuser et al. 2012a). These observations are consistent with a model in which the 1β dynein is the primary contributor to force production, and the 1α dynein is the motor domain that resists or limits microtubule sliding.

In another instance, mutations in the *BOP5* locus have defined an IC138 regulatory subcomplex within the I1 dynein (Fig. 3, inset) (Bower et al. 2009; Wirschell et al. 2009;

Heuser et al. 2012a). This subcomplex is also important for control of microtubule sliding, bend propagation, and the axonemal waveform (Brokaw and Kamiya 1987; Bayly et al. 2010; VanderWaal et al. 2011). Comparative analysis of the I1 structure between wild-type and *bop5* mutant axonemes by thin-section EM and cryo-ET confirmed the location of the IC138 complex at the proximal end of the 96-nm repeat, just above RS1 (Bower et al. 2009; Heuser et al. 2012a). In addition, as expected for a regulator of motility, cryo-ET analysis also revealed that the IC–LC complex of the I1 dynein interacts with multiple structures in the axoneme (Heuser et al. 2012a). These interactions include a link to the outer dynein arms, a link to inner-arm *a* (IA2), and a link to the MIA complex (Heuser et al. 2012a; Yamamoto et al. 2013). This IC–LC complex is thought to mediate signals to the two different I1 dynein motor domains, based in part on the phosphorylation state of the IC138 subunit.

3.4 Regulation of I1 Dynein by Axonemal Kinases and Phosphatases and IC138 Phosphorylation

In addition to its numerous structural interactions with other axonemal components (Heuser et al. 2012a), the activity of I1 dynein in the axoneme appears to be regulated by changes in phosphorylation of the intermediate chain subunit IC138 (Habermacher and Sale 1997; King and Dutcher 1997; Yang and Sale 2000; Bower et al. 2009; Wirschell et al. 2009). Although the mechanism of regulation by IC138 is not understood, the protein kinases (Yang and Sale 2000; Gaillard et al. 2001; Gokhale et al. 2009) and phosphatases thought to control IC138 phosphorylation (Elam et al. 2011) are physically anchored in the axoneme and are presumably in close proximity to IC138. The data support a model in which IC138 is the regulatory phosphoprotein that controls I1 dynein activity.

As mentioned above, the MIA complex contains two coiled-coiled proteins, FAP73 (MIA1) and FAP100 (MIA2), and both mutants show an altered waveform, slightly reduced beat frequency, and defective phototaxis—all of which are characteristic of defects in assembly and/or function of I1 dynein. Because the IC138 subunit was hyperphosphorylated in the *mia* mutants, the investigators postulated that the MIA complex exerts its regulatory effects through the kinases and phosphatases responsible for IC138 phosphorylation (Yamamoto et al. 2013). One model is that the MIA complex functions by correctly positioning the enzymes relative to the IC138 substrate to ultimately control ciliary waveform (King 2013; Yamamoto et al. 2013). In addition, the *mia* mutants show a slightly reduced beat frequency, suggesting a functional interaction between I1 and the outer arms (Yamamoto et al. 2013). Consistent with these observations,

cryo-ET has revealed a physical link between the IC–LC complex of I1 dynein and the outer dynein arm (Nicastro et al. 2006; Bui et al. 2009; Bui et al. 2012; Heuser et al. 2012a; Oda et al. 2013).

3.5 A Model for Local Control of Microtubule Sliding and Regulation of Ciliary Bending by I1 Dynein

One of the current questions concerns how the central pair/RS structures regulate the activity of I1 dynein. Structural evidence indicates that RSs can, in part, operate as mechanical transducers that can limit microtubule sliding (Warner and Satir 1974). Recent studies by Oda and colleagues (Oda et al. 2014b) indicate that a physical interaction between the spoke heads and central pair projections is required for regulating microtubule sliding and motility. One idea, illustrated in Figure 1, is that in wild-type axonemes, I1 activity is locally regulated by signals emanating from the central pair and directed to specific outer-doublet microtubules (Wargo and Smith 2003; Mitchell and Nakatsugawa 2004). In this model, signals, both chemical and mechanical in nature, from the asymmetric central pair are transmitted through the RSs to a specific subset of doublets, presumably on one side of the axis of the axoneme, to locally regulate I1 dynein activity (Fig. 1, curved red arrow). I1 dynein might act directly to regulate other dyneins or as a brake to impede sliding. Either way, the form of the bend would be altered, resulting in changes in the shape of the forward or the reverse bend or both (Porter and Sale 2000; Wirschell et al. 2007). Based on this general model and other features discussed in this section, a number of questions arise: What are the signals leading from the central pair to the outer doublets? How are signals from the central pair directed to specific outer doublets? How are signals from RS1 transmitted to the I1 dynein? Does the I1 dynein–MIA complex regulate the activity of other dyneins directly and/or operate as a “brake” to resist microtubule sliding?

4 THE RS2 REGULATORY COMPLEX AND DOWNSTREAM REGULATION

4.1 The Calmodulin- and Spoke-Associated Complex

The CSC was first identified as a group of three polypeptides that coimmunoprecipitated with calmodulin (CaM) and RS subunits in extracts prepared from wild-type axonemes (Dymek and Smith 2007). The calmodulin- and spoke-associated complex proteins (CaM-IP) polypeptides also cosedimented with the RS subunits at $\sim 20S$ on sucrose density gradients. However, when extracts were prepared from mutants lacking RS heads, the CSC subunits cosedi-

mented with the RS stalks at $\sim 17S$. Furthermore, when extracts from mutants lacking the RS were analyzed, the CSC subunits formed a smaller complex at $\sim 11S$. Blot overlay assays showed that one CSC subunit, CaM-IP2, binds directly to RSP3, an A-kinase anchoring protein (AKAP) located at the base of the RS stalk (Gaillard et al. 2001; Sivadas et al. 2012). Collectively, these data suggested that the CSC is tightly associated with the base of the RS stalk, but part of a distinct complex. However, it remained uncertain whether the CSC is associated with RS1 or RS2. A possible association with RS1 was suggested by the observation that treatment of central pair or RS mutant axonemes with an antibody against CaM-IP2 could increase microtubule sliding velocities, but only if the I1 dynein was also present (Dymek and Smith 2007). However, the coimmunoprecipitation of the CSC subunits with CaM was disrupted in the *drc* mutants *pf2* and *pf3*, suggesting a possible association with RS2. Resolution of this question would require the isolation of mutants that lack most of the CSC subunits.

The development of artificial microRNA (amiRNA) methods to knockdown expression of CaM-IP2 and -IP3 has resulted in the isolation of several strains that assemble reduced amounts of all three CSC subunits in isolated axonemes (Dymek et al. 2011). Biochemical comparisons further showed that CaM-IP2 and -IP3 correspond to RSP18 and -19, respectively, two RS subunits present in lower abundance than other RSPs (Yang et al. 2006; Heuser et al. 2012b). CSC amiRNA mutants swim forward with reduced swimming velocities owing to their shallow waveforms and a lack of coordination between their two flagella (Dymek et al. 2011). Assembly of the RS is variable and reduced when viewed by thin-section EM. Analysis by cryo-ET revealed that $\sim 50\%$ of the 96-nm repeats contain RS pairs, $\sim 25\%$ of the repeats lack RS2, and the remaining 96-nm repeats contain either an additional spoke or are too ambiguous to score. These observations strongly suggested that the CSC is associated with RS2 (Dymek et al. 2011). Subtomogram averaging further showed that the CSC mutants display variable defects in the structures of four other axonemal complexes in addition to RS2 (Fig. 4) (Heuser et al. 2012b). These include (1) the homolog of the third RS, known as RS3S; (2) some of the IDAs (IDA *e*, IA4; IDA *a*, IA2; and IDA *d*, IA6); (3) two regions of the N-DRC, one connecting to the tail of IDA *e* (IA4) and another connecting the N-DRC baseplate to RS2; and (4) a hole in the B-tubule inner junction near the base of RS2 and the N-DRC (Heuser et al. 2012b). Given the heterogeneity in RS assembly, the subtomogram averages were sorted into two classes, the first containing RS2 and the second lacking RS2. The class averages made it possible to identify those structural defects most closely correlated with the loss of CSC sub-

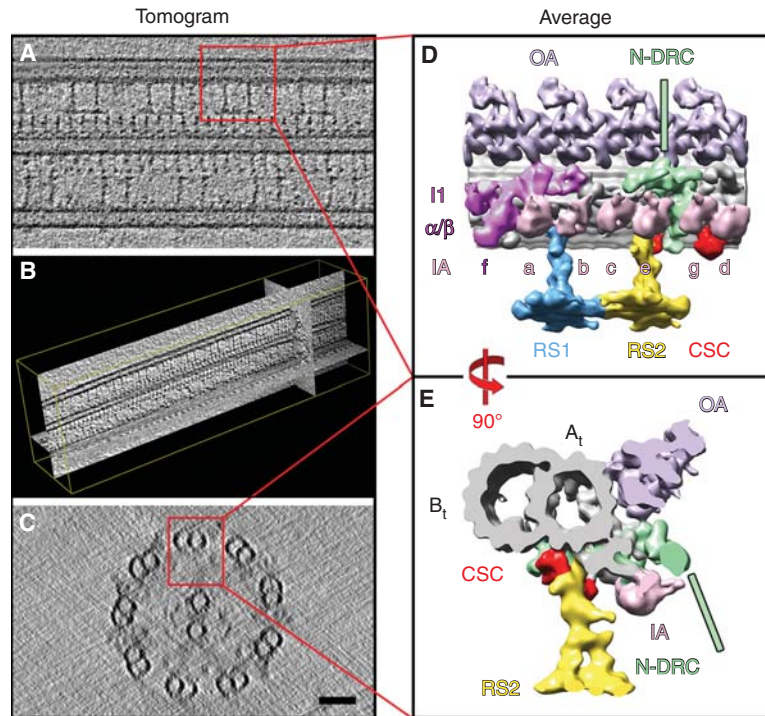


Figure 4. The *Chlamydomonas* axoneme ultrastructure. (A–C). Cryo-electron tomography slices show (A) a longitudinal view, (B) a 3D view, and (C) a cross section of a *Chlamydomonas* axoneme. The red boxes highlight one 96-nm axonemal repeat unit in both views. (D,E) Isosurface renderings show an averaged 96-nm axonemal repeat in (D) longitudinal and (E) cross-sectional orientation. The cross-sectional slice is taken close to radial spoke 2, viewing from the proximal to the distal end. Key axonemal structures are highlighted: A- and B-tubule (A_t , B_t), nexin–dynein regulatory complex (N-DRC), radial spokes (RS1,RS2), calmodulin- and spoke-associated complex (CSC), and inner and outer dynein arms (IA,OA). Inner-arm dyneins include the I1 complex (dynein f α and β heavy chain motor domains) and dyneins a–g. (Adapted from Satir et al. 2014; originally from Heuser et al. 2012b, with permission of the American Society for Cell Biology; permission conveyed through Copyright Clearance Center, Inc.; Heuser et al. 2012a.)

units. Comparisons with other RS and N-DRC mutants have led to the following model shown in Figure 4: the CSC subunits are located close to or within the two unique RS2 densities (the back prong of the RS2 base and the RS2-to-N-DRC connector), as well as part of RS3S (Heuser et al. 2012b). In addition, the CSC interacts with the baseplate of the N-DRC and physically interconnects the base of RS2 to the base of RS3S (see also Fig. 6 of Heuser et al. 2012b). How the individual CSC subunits might be arranged within these different structures is still unknown. Furthermore, there might be additional, as yet unidentified, subunits of the RS, N-DRC, and/or CSC that contribute to the assembly of this highly interconnected, regulatory hub.

4.2 Genetic Analyses of the Dynein Regulatory Complex

Early efforts to identify other components involved in signaling between the RS and the dynein arms were based on the observation that most RS and CP mutations resulted in

flagellar paralysis. The isolation of extragenic suppressors that could restore some motility to RS/CP mutants resulted in the identification of five loci, known as *SUP-PF1–SUP-PF5* (Huang et al. 1982; Piperno et al. 1994). Double-mutant analyses showed that two motility mutants, *pf2* and *pf3*, could also suppress RS/CP paralysis (Huang et al. 1982). Molecular and biochemical studies sorted the seven loci into two groups, one group that alters the activity of the outer dynein arms and flagellar beat frequency, and a second group that appears to alter the activity of the IDAs and the flagellar waveform (Huang et al. 1982; Brokaw and Kamiya 1987; Piperno et al. 1992; Gardner et al. 1994). The first group is represented by the *sup-pf1* and *sup-pf2* alleles in the genes encoding the β and γ DHCs, respectively, of the outer dynein arm (Porter et al. 1994; Rupp et al. 1996). The *sup-pf1* and *sup-pf2* mutations specifically reduce outer dynein arm activity, but they do not block assembly of the outer dynein arm. These observations led to a model in which the CP/RS are predicted to coordinate dynein activity by selectively stimulating the inner-arm dy-

neins. In the absence of signals from the CP/RS, the IDAs are partially inhibited, leading to flagellar paralysis. However, motility can be restored either by mutations that stimulate inner-arm activity or by mutations that reduce outer-arm activity.

The second group of mutations did not directly affect dynein arms, but were instead associated with defects in the assembly of a discrete subset of tightly bound axonemal proteins known as the dynein regulatory complex (DRC) (Huang et al. 1982; Piperno et al. 1992; Piperno et al. 1994). The precise location of the DRC subunits was initially unknown, but Brokaw and Kamiya (1987) noted that *drc* mutants displayed aberrant flagellar waveforms similar to those observed in inner-arm dynein mutants. Biochemical studies later confirmed that many *drc* mutants were also deficient in the assembly of a subset of inner-arm dyneins (Piperno et al. 1992; Gardner et al. 1994; Piperno et al. 1994). Comparison of wild-type and mutant axonemes by thin-section EM and computer-image averaging finally revealed that most *drc* mutants lacked a large, crescent-shaped structure at the distal end of the 96-nm repeat (Mastronarde et al. 1992; Gardner et al. 1994; Rupp and Porter 2003). Interestingly, this structure was located at the junction between the inner and outer dynein arms and RS2, ideally situated to mediate signals between these structures (Fig. 2). Mastronarde and colleagues noted that this location was close to the predicted attachment site of the nexin link, but the precise relationship between the DRC and the nexin link remained uncertain (Mastronarde et al. 1992).

4.3 Identification of the DRC as the Nexin Link

Early EM studies identified the nexin links as flexible filaments that interconnect the A tubule of one outer doublet microtubule to the B tubule of the adjacent outer doublet. They were first described in extracted *Tetrahymena* axonemes (Gibbons 1963) and then visualized in intact cilia following ninefold rotation of axoneme cross sections. Their presence in extracted ciliary remnants led to the proposal that the nexin links are crucial for maintaining the cylindrical structure of the nine doublet microtubules within the axoneme (Stephens 1970).

Analysis of longitudinal sections indicated that the nexin links repeat every 96 nm and are often inclined at variable angles (Warner 1976; Witman et al. 1978). Under experimental conditions that induced outer doublet microtubules to splay apart, the nexin links appeared to stretch (Warner 1976). However, other studies of actively bending axonemes suggested instead that the nexin links undergo cycles of lateral displacement along the B tubule (Warner 1983; Bozkurt and Woolley 1993; Woolley 1997).

The study of actively beating flagella by cryo-ET (Lin et al. 2014a) might soon resolve this apparent discrepancy.

The idea that the nexin links are the essential component that resists dynein-driven microtubule sliding was based on early studies with protease-treated axonemes. EM analysis of isolated axonemes indicated that protease treatment disrupted the nexin links and RSs with a time-course that could be correlated closely with the extent of ATP-induced axoneme disintegration (Summers and Gibbons 1971). Furthermore, *pf14* axonemes lacking RSs would not undergo microtubule sliding without protease treatment (Witman et al. 1978). These observations implicated the nexin links as the protease-sensitive structure resisting dynein activity.

Cryo-ET has resolved some of the mysteries associated with the nexin link. Images of wild-type axonemes showed that the nexin link is a very large structure (~1.5 MDa), with one end anchored to the A tubule, close to the base of RS2. The link wraps around the A tubule and then bifurcates as it reaches across the interdoublt space to make contact with the neighboring B tubule (Figs. 4 and 5) (Nicastro et al. 2006).

Later studies revealed that the various *drc* mutants lack different regions within the overall structure of the nexin link (Heuser et al. 2009). The missing regions define two major domains—the baseplate and the linker (Fig. 5). The baseplate is the region attached to the underside of the A tubule, extending from the A tubule–B tubule junction to protofilament A4 of the A tubule. This domain is ~350 kDa, and it is significantly reduced in the *pf3* mutant. The baseplate also makes at least three connections to neighboring structures in the axoneme. These include (1) a thin connection between the end of the baseplate and the B11 protofilament adjacent to the A tubule–B tubule junction, (2) a connection between the baseplate and the tail of inner-arm dynein *e* (IA4), and (3) a connection between the baseplate and RS2. As discussed above (Fig. 4), the subunits of the CSC are likely to contribute to the connection between the baseplate and RS2 and might also connect the baseplate to RS3S (Heuser et al. 2009; Heuser et al. 2012b). The DRC linker begins approximately at protofilament A4 and extends toward the B tubule of the neighboring outer doublet (Fig. 5). It is a very large structure (~1.2 MDa) and contains several subdomains. One subdomain is a protrusion that connects the DRC to the outer dynein arms known as OID2 (Fig. 4). Chemical cross-linking studies suggest that this linker involves a direct interaction between DRC4 and IC2 (IC69) of the outer-arm dynein (Oda et al. 2013). A second subdomain is a protrusion that connects the DRC to dynein *g* (IA5). This protrusion is defective in the *drc3* (*fap134*) mutant (Awata et al. 2015). As the DRC linker reaches across the interdoublt

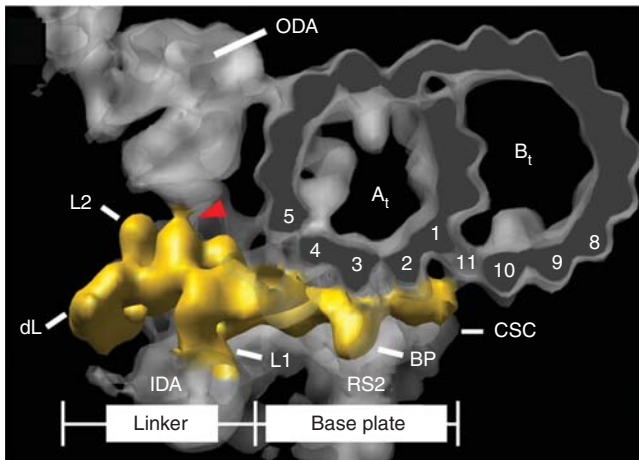


Figure 5. Cryo-electron tomography (cryo-ET) reconstruction of the nexin–dynein regulatory complex (N-DRC). This image shows the N-DRC in yellow, as viewed from the distal end of a 96-nm axoneme repeat in cross section. A single outer doublet is shown here, with a subset of protofilaments numbered in the A tubule (A_t) and B tubule (B_t). The outer dynein arms (ODA) are shown in gray at the *top left*, and one of the inner dynein arms (IDA) is shown in gray at the *bottom left*. The baseplate of the N-DRC is attached to protofilament 11 on the B tubule and wraps around the underside of the A tubule until protofilament 4. The linker of the N-DRC extends from the surface of the A tubule toward the neighboring outer doublet, and it also contacts both the IDA (at L1) and the ODA (red arrowhead). Radial spoke 2 (RS2) attaches to the A tubule just behind the N-DRC. The calmodulin- and spoke-associated complex (CSC) sits at the base of RS2 and wraps around the N-DRC to the next RS3 or RS3S, which is not shown here. The precise boundaries among the subunits of RS2, the CSC, and the base of the DRC are not well defined. (Adapted from Heuser et al. 2009.)

space, it branches into two other subdomains—proximal and distal (Figs. 4 and 5). Interestingly, both the proximal and distal subdomains make contact with protofilament B8 of the neighboring B tubule. These observations suggest that the alignment of the DRC with the neighboring outer doublet is quite precise, as compared with the dynein arms, which contact several different B-tubule protofilaments (Lin et al. 2014a).

Nearly all of the DRC linker is missing in *pf2* and *sup-pf3* axonemes, and a major portion is also missing in *pf3*. Given that the DRC linker is the only structure that interconnects the outer doublets besides the dynein arms, the obvious conclusion is that the DRC is part of the nexin link (Heuser et al. 2009). However, given that most investigators have assumed that the nexin link is essential for axoneme integrity, it was surprising that none of the existing *drc* mutants showed any obvious defects in the arrangement of outer doublet microtubules. These observations suggested that other components remaining in the *drc* mutants are sufficient to maintain axoneme integrity *in vivo*.

Interestingly, mutations in two new genes that affect the assembly of DRC subunits have been identified recently in dogs, zebrafish, and humans (Becker-Heck et al. 2011; Merveille et al. 2011). These mutations disrupt the genes encoding two highly conserved, coiled-coil proteins known as CCDC39 and CCDC40 in vertebrates. Although the biochemical defects have not been well characterized in vertebrates, both mutants have obvious structural defects in the assembly of IDAs and the DRC. In addition, mutations in both genes are associated with varying degrees of microtubule disorganization within the axoneme. The *Chlamydomonas* orthologs of CCDC40 and CCDC39—FAP172 and FAP59—were recently identified as the defective gene products in *pf7* and *pf8*, respectively (Lin et al. 2015). Loss of these proteins in *pf7* and *pf8* mutant axonemes disrupts the assembly of several IDAs and N-DRC subunits (Lin et al. 2015). By tagging the amino- and carboxy-terminal domains of FAP172 and FAP59 and transforming the tagged constructs into the *pf7* and *pf8* mutants, Oda and colleagues (Oda et al. 2014a) determined that these proteins form a long, extended structure that serves as a molecular “ruler” to define the 96-nm repeat and mark the locations of specific binding sites for several IDAs, the RSs, and the N-DRC (Oda et al. 2014a). Additional work is needed to determine how each of these complexes is docked to its appropriate location.

4.4 DRC Subunit Composition and Function

Analysis by one-dimensional (1D) and two-dimensional (2D) gel electrophoresis identified seven polypeptides that are missing to varying degrees in the *drc* mutants (Table 4) (Huang et al. 1982; Piperno et al. 1992; Piperno et al. 1994). DRC4 was first identified by rescue of a *pf2* mutation that had been tagged by plasmid insertion, and corresponds to a highly conserved, coiled-coil protein of ~55 kDa, which is ubiquitous in organisms with motile axonemes (Rupp and Porter 2003). As mentioned above, *pf2* mutants in *Chlamydomonas* have defects in the assembly of the DRC linker (Fig. 5). Transformation with both wild-type and epitope-tagged versions of PF2/DRC4 restores motility and all of the missing polypeptides and structures (Rupp and Porter 2003; Heuser et al. 2009; Bower et al. 2013). These results suggest that DRC4 plays a crucial role in the assembly of the DRC linker domain. This hypothesis is further supported by studies on an unusual DRC4 mutation known as *sup-pf3* (Bower et al. 2013). The *sup-pf3* mutant is the result of transposon insertion into the *DRC4* gene, resulting in alternate splicing and in-frame deletions within the *DRC4* coding sequence. The truncated DRC4 subunits assemble into the axoneme, but most of the linker polypeptides are still missing

Table 4. Nexin–dynein regulatory complex (N-DRC) proteins

| <i>Chlamydomonas</i> name | MW (kDa) | Motifs | Missing or reduced in mutant | <i>Homo sapiens</i> | References |
|---------------------------|----------|-------------|---------------------------------|---------------------|--|
| DRC1 | 79 | Coiled-coil | <i>pf3</i> | CCDC164 | Wirschell et al. 2013 |
| DRC2 (FAP250) | 65 | Coiled-coil | <i>pf3, ida6</i> | CCDC65 | Lin et al. 2011; Bower et al. 2013; Austin-Tse et al. 2013 |
| DRC3 (FAP134) | 60 | LRR | <i>pf2, sup-pf3, drc3</i> | LRRC48 | Lin et al. 2011; Bower et al. 2013; Awata et al. 2015 |
| DRC4 (PF2) | 55 | Coiled-coil | <i>pf2, sup-pf3</i> | GAS11 | Rupp and Porter 2003 |
| DRC5 (FAP155) | 43 | LRR | all except <i>drc3</i> | TCTE1 | Lin et al. 2011; Bower et al. 2013 |
| DRC6 (FAP169) | 28 | – | all except <i>drc3</i> | FBXL13 | Lin et al. 2011; Bower et al. 2013 |
| DRC7 (FAP50) | 177 | LRR, TGL | all except <i>sup-pf4, drc3</i> | CCDC135 | Lin et al. 2011; Bower et al. 2013 |
| DRC8 (FAP200) | 19 | EF hand | all except <i>sup-pf4, drc3</i> | EFCBD2 | Bower et al. 2013 |
| DRC9 (FAP122) | 46 | IQ | all except <i>sup-pf4, drc3</i> | IQCG | Bower et al. 2013 |
| DRC10 (FAP84) | 41 | IQ | all except <i>sup-pf4, drc3</i> | IQCD | Bower et al. 2013 |
| DRC11 (FAP82) | 95 | AAA, IQ | all except <i>sup-pf4, drc3</i> | IQCA1 | Bower et al. 2013 |

MW, molecular weight; AAA, “ATPases associated with diverse cellular activities” motif; EF hand, Ca²⁺-binding motif; IQ, IQ calmodulin-binding motif; LRR, leucine-rich repeat; DRC, dynein regulatory complex; TGL, transglutaminase-like.

(Table 4). The structures that remain are the baseplate and a small domain at the base of the linker region, close to the A tubule (Heuser et al. 2009). These observations and other studies indicating that DRC4 can be chemically cross-linked to the outer dynein arm subunit IC2 (Oda et al. 2013) have led to a model that predicted that a portion of DRC4 is located close to the base of the DRC linker. Tagging of DRC4 subunits at several sites followed by cryo-ET localization of tagged DRC4 constructs has recently revealed that DRC4 is an elongated coiled-coil protein that extends from one end of the baseplate to the end of the linker region (Oda et al. 2015; Song et al. 2015).

Studies of DRC4 orthologs in other species indicate that this subunit plays a conserved role in ciliary and flagellar motility. For instance, RNA interference (RNAi)-mediated knockdown of a trypanosome ortholog known as trypanin has shown that this protein is required for optimal flagellar motility and is essential for viability of the bloodstream form of the parasite that causes sleeping sickness (Ralston and Hill 2006). DRC4 is also essential for ciliary motility in vertebrates. Known as GAS11 in humans and GAS8 in mice and zebrafish, the vertebrate ortholog was first described as a gene in mouse fibroblasts whose expression was stimulated by serum starvation and growth arrest. These observations prompted several investigators to search for a role for DRC4/Gas8/Gas11 in primary cilia, but thus far the evidence has been inconclusive (reviewed in Porter 2012). However, knockdown of GAS8 in zebrafish results in hydrocephaly, neural tube cell death, left–right axis defects, and defects in otolith biogenesis—all phenotypes associated with defects in ciliary motility (Colantoni et al. 2009). Mutations in *DRC4/GAS11* have recently

been found in three patients with primary ciliary dyskinesia (PCD) (Olbrich et al. 2015).

Mutations in DRC1 and DRC2 have also recently been identified in *Chlamydomonas* and human patients with PCD (Austin-Tse et al. 2013; Wirschell et al. 2013). In *Chlamydomonas*, DRC1 is the *PF3* gene product, and the *pf3* mutation is a premature stop codon that truncates the DRC1 protein after six amino acids (Wirschell et al. 2013). The mutant DRC1 polypeptide fails to assemble into the axoneme, and most of the other DRC subunits are also missing or reduced (Table 4). Consistent with these observations, the *pf3* mutant fails to assemble most of the baseplate and DRC linker (Fig. 5) (Heuser et al. 2009). The defects impact connections to other structures within this region. For example, several of the inner-arm dyneins most closely associated with RS2 are reduced (Gardner et al. 1994; Heuser et al. 2009; Wirschell et al. 2013). In addition, interactions between the base of RS2 and the CSC appear to be disrupted (Fig. 4) (Heuser et al. 2009; Dymek et al. 2011; Heuser et al. 2012b). Tagging of DRC1 followed by cryo-ET localization of *DRC1* constructs has shown that DRC1 also extends from one end of the baseplate to the end of the linker region (Oda et al. 2015).

Similar to DRC4, DRC1 is a highly conserved, coiled-coil protein that appears to be ubiquitous in organisms with motile axonemes (Bower et al. 2013; Wirschell et al. 2013). The vertebrate ortholog is known as CCDC164, and mutations in this sequence have been linked to PCD in at least three families (Wirschell et al. 2013). The *ccdc164* mutations reduce the amplitude of the ciliary beat in isolated respiratory cilia and also disrupt the assembly of the nexin links and at least two DRC subunits. Interestingly,

however, the organization of microtubules within the axoneme is relatively normal, and CCDC39 is also present, similar to the *Chlamydomonas pf3* mutant. These observations indicate that the phenotypes of typical *drc* mutations in human patients can be extremely subtle and potentially easy to overlook by conventional transmission electron microscopy (TEM) in the absence of careful analysis of the ciliary waveforms (Wirschell et al. 2013).

The remaining DRC subunits have been identified by a combination of 2D gel electrophoresis, immunoprecipitation, labeling by a technique known as “isobaric tag for relative and absolute quantitation” (iTRAQ) and mass spectrometry (Table 4) (Lin et al. 2011; Bower et al. 2013). The efforts have resulted in the characterization of nine additional subunits, although it is highly likely that there are others yet to be identified.

DRC2 is another highly conserved coiled-coil polypeptide known as FAP250 in *Chlamydomonas*, CCDC65 in vertebrates, and CMF70 in trypanosomes (Kabutu et al. 2010; Austin-Tse et al. 2013). Its sequence is closely related to DRC1/CCDC164, and the two proteins appear to interact based on their coassembly in *pf2*, *sup-pf3*, and *sup-pf4* and their absence in *pf3* and *sup-pf5* (Table 4). Recent work has identified DRC2 as the mutant gene product of the *IDA6* locus (Austin-Tse et al. 2013). The *ida6* mutant was first identified as an inner-arm motility mutant lacking dynein *e*, similar to *pf3* (Kato 1993; Gardner et al. 1994). Later studies revealed that the tektin polypeptide, thought to be a component of the A-tubule protofilament ribbon, is also significantly reduced in *ida6*, *pf3*, and *sup-pf5* (Yanagisawa and Kamiya 2004). These observations prompted a reevaluation of the *ida6* mutant by thin-section TEM and image averaging. This approach revealed that *ida6* also has significant defects in DRC structure that can be rescued by transformation with wild-type DRC2 (Austin-Tse et al. 2013). Tagging and localization of DRC2 subunits has further shown that DRC2 also extends from the baseplate to the linker region, similar to DRC1 and DRC4 (Oda et al. 2015). Additional work is needed to characterize the full extent of the structural and biochemical defects in *ida6*, but studies in other species have confirmed that DRC2 orthologs play a conserved role in motility. Knockdown of CCDC65 and CMF70 in zebrafish and trypanosomes alters the ciliary and flagellar beat patterns, and mutations in CCDC65 have been linked to PCD in at least three families (Kabutu et al. 2010; Austin-Tse et al. 2013; Horani et al. 2013).

DRC3 is known as FAP134 in *Chlamydomonas* and the leucine-rich repeat (LRR) protein LRRC48 in vertebrates (Lin et al. 2011; Bower et al. 2013). A *drc3* mutant has been identified in *Chlamydomonas* (Lechtreck et al. 2009). Loss of DRC3 disrupts the assembly of IDA g, but it has minimal

effects on the assembly of other N-DRC subunits (Awata et al. 2015). However, DRC3 appears to be closely associated with DRC4, based on its assembly with truncated DRC4 subunits in *sup-pf3* and its absence in the DRC4-null mutant *pf2* (Bower et al. 2013; Alford et al. 2016). Tagging of DRC3 and localization by cryo-ET has shown that DRC3 is an important component of the protrusion that connects the linker region to IDA g (Song et al. 2015).

DRC5 (FAP155) and DRC6 (FAP169) are subunits associated with the distal region of the linker domain that makes contact with the neighboring B tubule (Figs. 4 and 5). This conclusion is based on the structural and biochemical phenotypes of the *sup-pf4* mutant, which lacks only two polypeptides and a small portion of the distal linker (Huang et al. 1982; Piperno et al. 1992; Gardner et al. 1994; Piperno et al. 1994; Heuser et al. 2009). More recent work has shown that the *sup-pf4* mutation is a large deletion that removes DRC5 and two neighboring genes (Lin et al. 2011). The loss of DRC5 and DRC6 partially destabilizes the isolated DRC in *sup-pf4* extracts, but transformation with DRC5-HA rescues the mutant and restabilizes the DRC (Bower et al. 2013). It is not known which subunit makes direct contact with the B tubule. The carboxyl terminus of DRC5 is located near the base of the linker, as determined by cryo-ET localization of a tagged construct (Oda et al. 2015), but the amino terminus has not yet been localized. However, the DRC5 (FAP155) sequence is a LRR protein that is significantly more highly conserved in other species with motile axonemes than the DRC6 (FAP169) sequence, and so DRC5 (FAP155) seems to be the more likely candidate (Bower et al. 2013). No mutations have been described in other species, but, given the subtle motility defects observed with *sup-pf4* in *Chlamydomonas*, such mutations might be difficult to detect.

At ~177 kDa, DRC7 is the largest known subunit of the DRC, and it contains several conserved domains, including LRR sequences in the amino-terminal third of the polypeptide. However, the most highly conserved region is the carboxy-terminal third of the polypeptide, which contains the recently identified transglutaminase-like (TGL) peptidase domain (Zhang and Aravind 2012). This motif is conserved in both the *Drosophila* ortholog CG34110 and the vertebrate ortholog CCDC135, and it is predicted to bind tightly to glutamylated proteins. Because DRC7/FAP50 appears to be a major component of the linker region, it is tempting to speculate that the TGL domain facilitates interactions with glu-tubulin residues on the B tubule. Studies of glutamylation-defective mutants (*tpg1*, *tpg2*) in *Chlamydomonas* have indicated that microtubule sliding is altered in these strains (Kubo et al. 2010). Although no DRC7/FAP50 mutations have been identified in *Chlamydomonas*, a mutation in the *Drosophila* ortholog

CG34110 known as *lost boys (lobo)* is associated with defects in the movement of sperm in the female reproductive tract (Yang et al. 2011). This movement is a Ca^{2+} -regulated process that requires changes in the flagellar waveform and in the direction of wave propagation. As no Ca^{2+} -binding domain has been identified in DRC7, it seems likely that some other Ca^{2+} -binding proteins are also involved in this process.

The DRC8–DRC11 subunits contain either Ca^{2+} - or CaM-binding domains, suggesting that they contribute to one of the many pathways that modulate flagellar motility in response to changes in intracellular Ca^{2+} (Bower et al. 2013). DRC11 also contains an AAA domain that could potentially mediate nucleotide-sensitive conformational changes. These subunits are reduced in all of the *drc* mutants except *sup-pf4*, but little is yet known about their specific interactions or locations within the larger structure of the N-DRC (Bower et al. 2013). Additional work is needed to understand how they fit within the network of mechanochemical signals transmitted from the RS heads to the RS stalk, from the RS stalk to the CSC and N-DRC, and from the N-DRC to multiple inner-arm dyneins. The isolation and identification of selective mutations in all of the N-DRC subunits will be an essential next step for the dissection of this complex regulatory hub.

The presence of several DRC subunits in organisms with motile axonemes that lack the CP, RS, and IDAs (Bower et al. 2013) also suggests a more basic function for the N-DRC beyond the higher-order control of waveform provided by the RS/CP system. An intriguing possibility is that the N-DRC plays a crucial role in maintaining the outer-doublet alignment in motile 9 + 0 axonemes. This hypothesis is consistent with the presence of the nexin links in extracted ciliary remnants first described more than 40 years ago and more recent work indicating that loss of the N-DRC increases the splaying of outer doublets in isolated, ATP-treated axonemes (Bower et al. 2013; Alford et al. 2016). The further study of motile 9 + 0 axonemes might shed additional light on the functions of the N-DRC.

5 CONCLUSION

Comparative genomics and proteomics have revealed that ciliary and flagellar axonemes contain more than 500 proteins. Although significant progress has been made in assigning many of these proteins to specific structures, more than half of these proteins are still uncharacterized. Recent work featured in this review has revealed two important regulatory hubs within the 96-nm repeat that interconnect several of the most well-characterized axoneme components. Additional work using specifically tagged subunits is still needed to understand how these different structures

interact. New biophysical tools, including optical approaches, are also required so that we can test the various models for how the axonemal subcomplexes work together in vivo to generate motility.

ACKNOWLEDGMENTS

This work was supported by a predoctoral fellowship from the American Heart Association (AHA-11PRE7440043 to R.V.) and grants from the National Institutes of Health (NIH) (GM-051173 to W.S.S.; GM-055667 to M.E.P.).

REFERENCES

- Ahmed NT, Mitchell DR. 2005. ODA16p, a *Chlamydomonas* flagellar protein needed for dynein assembly. *Mol Biol Cell* **16**: 5004–5012.
- Alford LM, Stoddard D, Li JH, Hunter EL, Tritschler D, Bower R, Nicastro D, Porter ME, Sale WS. 2016. The nexin link and B-tubule glutamylation maintain the alignment of outer doublets in the ciliary axoneme. *Cytoskeleton* **73**: 331–340.
- Austin-Tse C, Halbritter J, Zariwala MA, Gilberti RM, Gee HY, Hellman N, Pathak N, Liu Y, Panizzi JR, Patel-King RS, et al. 2013. Zebrafish ciliopathy screen plus human mutational analysis identifies C21orf59 and CCDC65 defects as causing primary ciliary dyskinesia. *Am J Hum Genet* **93**: 672–686.
- Awata J, Song K, Lin J, King SM, Sanderson MJ, Nicastro D, Witman GB. 2015. DRC3 connects the N-DRC to dynein g to regulate flagellar waveform. *Mol Biol Cell* **26**: 2788–2800.
- Barber CF, Heuser T, Carbajal-Gonzalez BI, Botchkarev VV Jr, Nicastro D. 2012. Three-dimensional structure of the radial spokes reveals heterogeneity and interactions with dyneins in *Chlamydomonas* flagella. *Mol Biol Cell* **23**: 111–120.
- Bayly PV, Lewis BL, Kemp PS, Pless RB, Dutcher SK. 2010. Efficient spatiotemporal analysis of the flagellar waveform of *Chlamydomonas reinhardtii*. *Cytoskeleton* **67**: 56–69.
- Becker-Heck A, Zohn IE, Okabe N, Pollock A, Lenhart KB, Sullivan-Brown J, McSheene J, Loges NT, Olbrich H, Haeffner K, et al. 2011. The coiled-coil domain containing protein CCDC40 is essential for motile cilia function and left–right axis formation. *Nat Genet* **43**: 79–84.
- Bower R, Vanderwaal K, O’Toole E, Fox L, Perrone C, Mueller J, Wirschell M, Kamiya R, Sale WS, Porter ME. 2009. IC138 defines a sub-domain at the base of the I1 dynein that regulates microtubule sliding and flagellar motility. *Mol Biol Cell* **20**: 3055–3063.
- Bower R, Tritschler D, Vanderwaal K, Perrone CA, Mueller J, Fox L, Sale WS, Porter ME. 2013. The N-DRC forms a conserved biochemical complex that maintains outer doublet alignment and limits microtubule sliding in motile axonemes. *Mol Biol Cell* **24**: 1134–1152.
- Bozkurt HH, Woolley DM. 1993. Morphology of nexin links in relation to interdoublet sliding in the sperm flagellum. *Cell Motil Cytoskeleton* **24**: 109–118.
- Brokaw CJ. 1985. Computer simulation of flagellar movement. VI. Simple curvature-controlled models are incompletely specified. *Biophys J* **48**: 633–642.
- Brokaw CJ. 1989. Direct measurements of sliding between outer doublet microtubules in swimming sperm flagella. *Science* **243**: 1593–1596.
- Brokaw CJ. 2009. Thinking about flagellar oscillation. *Cell Motil Cytoskeleton* **66**: 425–436.
- Brokaw CJ, Kamiya R. 1987. Bending patterns of *Chlamydomonas* flagella: IV. Mutants with defects in inner and outer dynein arms indicate differences in dynein arm function. *Cell Motil Cytoskeleton* **8**: 68–75.

- Bui KH, Ishikawa T. 2013. 3D structural analysis of flagella/cilia by cryo-electron tomography. *Methods Enzymol* **524**: 305–323.
- Bui KH, Sakakibara H, Movassagh T, Oiwa K, Ishikawa T. 2009. Asymmetry of inner dynein arms and inter-doublet links in *Chlamydomonas* flagella. *J Cell Biol* **186**: 437–446.
- Bui KH, Yagi T, Yamamoto R, Kamiya R, Ishikawa T. 2012. Polarity and asymmetry in the arrangement of dynein and related structures in the *Chlamydomonas* axoneme. *J Cell Biol* **198**: 913–925.
- Casey DM, Inaba K, Pazour GJ, Takada S, Wakabayashi K, Wilkerson CG, Kamiya R, Witman GB. 2003. Dc3, the 21-kDa subunit of the outer arm-docking complex (ODA-DC), is a novel EF-hand protein important for the assembly of both the outer arm and ODA-DC. *Mol Biol Cell* **14**: 3650–3663.
- Carbajal-Gonzalez BI, Heuser T, Fu X, Lin J, Smith BW, Mitchell DR, Nicastro D. 2013. Conserved structural motifs in the central pair complex of eukaryotic flagella. *Cytoskeleton* **70**: 101–120.
- Colantonio JR, Vermont J, Wu D, Langenbacher AD, Fraser S, Chen JN, Hill KL. 2009. The dynein regulatory complex is required for ciliary motility and otolith biogenesis in the inner ear. *Nature* **457**: 205–209.
- Curry AM, Williams BD, Rosenbaum JL. 1992. Sequence analysis reveals homology between two proteins of the flagellar radial spoke. *Mol Cell Biol* **12**: 3967–3977.
- Dean AB, Mitchell DR. 2013. *Chlamydomonas* ODA10 is a conserved axonemal protein that plays a unique role in outer dynein arm assembly. *Mol Biol Cell* **24**: 3689–3696.
- DiBella LM, Benashski SE, Tedford HW, Harrison A, Patel-King RS, King SM. 2001. The Tctex1/Tctex2 class of dynein light chains. Dimerization, differential expression, and interaction with the LC8 protein family. *J Biol Chem* **276**: 14366–14373.
- DiBella LM, Sakato M, Patel-King RS, Pazour GJ, King SM. 2004a. The LC7 light chains of *Chlamydomonas* flagellar dyneins interact with components required for both motor assembly and regulation. *Mol Biol Cell* **15**: 4633–4646.
- DiBella LM, Smith EF, Patel-King RS, Wakabayashi K, King SM. 2004b. A novel Tctex2-related light chain is required for stability of inner dynein arm II and motor function in the *Chlamydomonas* flagellum. *J Biol Chem* **279**: 21666–21676.
- DiBella LM, Gorbatyuk O, Sakato M, Wakabayashi K, Patel-King RS, Pazour GJ, Witman GB, King SM. 2005. Differential light chain assembly influences outer arm Dynein motor function. *Mol Biol Cell* **16**: 5661–5674.
- Duriez B, Duquesnoy P, Escudier E, Bridoux AM, Escalier D, Rayet I, Marcos E, Vojtek AM, Bercher JF, Amselem S. 2007. A common variant in combination with a nonsense mutation in a member of the thio-redoxin family causes primary ciliary dyskinesia. *Proc Natl Acad Sci* **104**: 3336–3341.
- Dutcher SK. 2014. The awesome power of dikaryons for studying flagella and basal bodies in *Chlamydomonas reinhardtii*. *Cytoskeleton* **71**: 79–94.
- Dymek EE, Smith EF. 2007. A conserved CaM- and radial spoke associated complex mediates regulation of flagellar dynein activity. *J Cell Biol* **179**: 515–526.
- Dymek EE, Heuser T, Nicastro D, Smith EF. 2011. The CSC is required for complete radial spoke assembly and wild-type ciliary motility. *Mol Biol Cell* **22**: 2520–2531.
- Elam CA, Wirschell M, Yamamoto R, Fox LA, York K, Kamiya R, Dutcher SK, Sale WS. 2011. An axonemal PP2A B-subunit is required for PP2A localization and flagellar motility. *Cytoskeleton* **68**: 363–372.
- Freshour J, Yokoyama R, Mitchell DR. 2007. *Chlamydomonas* flagellar outer row dynein assembly protein ODA7 interacts with both outer row and II inner row dyneins. *J Biol Chem* **282**: 5404–5412.
- Gaillard AR, Diener DR, Rosenbaum JL, Sale WS. 2001. Flagellar radial spoke protein 3 is an A-kinase anchoring protein (AKAP). *J Cell Biol* **153**: 443–448.
- Gardner LC, O'Toole E, Perrone CA, Giddings T, Porter ME. 1994. Components of a "dynein regulatory complex" are located at the junction between the radial spokes and the dynein arms in *Chlamydomonas* flagella. *J Cell Biol* **127**: 1311–1325.
- Gibbons IR. 1963. Studies on the protein components of cilia from *Tetrahymena pyriformis*. *Proc Natl Acad Sci* **50**: 1002–1010.
- Gibbons BH, Gibbons IR. 1972. Flagellar movement and adenosine triphosphatase activity in sea urchin sperm extracted with triton X-100. *J Cell Biol* **54**: 75–97.
- Gibbons BH, Gibbons IR. 1973. The effect of partial extraction of dynein arms on the movement of reactivated sea-urchin sperm. *J Cell Sci* **13**: 337–357.
- Gokhale A, Wirschell M, Sale WS. 2009. Regulation of dynein-driven microtubule sliding by the axonemal protein kinase CK1 in *Chlamydomonas* flagella. *J Cell Biol* **186**: 817–824.
- Goodenough UW, Heuser JE. 1982. Substructure of the outer dynein arm. *J Cell Biol* **95**: 798–815.
- Goodenough UW, Heuser JE. 1985. Substructure of inner dynein arms, radial spokes, and the central pair/projection complex of cilia and flagella. *J Cell Biol* **100**: 2008–2018.
- Habermacher G, Sale WS. 1997. Regulation of flagellar dynein by phosphorylation of a 138-kD inner arm dynein intermediate chain. *J Cell Biol* **136**: 167–176.
- Harris EH. 2009. *The Chlamydomonas sourcebook: Introduction to Chlamydomonas and its laboratory use*. Academic, Oxford.
- Harrison A, Olds-Clarke P, King SM. 1998. Identification of the *t* complex-encoded cytoplasmic dynein light chain tctex1 in inner arm II supports the involvement of flagellar dyneins in meiotic drive. *J Cell Biol* **140**: 1137–1147.
- Hayashi S, Shingyoji C. 2008. Mechanism of flagellar oscillation-bending-induced switching of dynein activity in elastase-treated axonemes of sea urchin sperm. *J Cell Sci* **121**: 2833–2843.
- Hendrickson TW, Perrone CA, Griffin P, Wuichet K, Mueller J, Yang P, Porter ME, Sale WS. 2004. IC138 is a WD-repeat dynein intermediate chain required for light chain assembly and regulation of flagellar bending. *Mol Biol Cell* **12**: 5431–5442.
- Heuser T, Raytchev M, Krell J, Porter ME, Nicastro D. 2009. The dynein regulatory complex is the nexin link and a major regulatory node in cilia and flagella. *J Cell Biol* **187**: 921–933.
- Heuser T, Barber CF, Lin J, Krell J, Rebesco M, Porter ME, Nicastro D. 2012a. Cryoelectron tomography reveals doublet-specific structures and unique interactions in the II dynein. *Proc Natl Acad Sci* **109**: E2067–E2076.
- Heuser T, Dymek EE, Lin J, Smith EF, Nicastro D. 2012b. The CSC connects three major axonemal complexes involved in dynein regulation. *Mol Biol Cell* **23**: 3143–3155.
- Hirono M, Uryu S, Ohara A, Kato-Minoura T, Kamiya R. 2003. Expression of conventional and unconventional actins in *Chlamydomonas reinhardtii* upon deflagellation and sexual adhesion. *Eukaryot Cell* **2**: 486–493.
- Hom EF, Witman GB, Harris EH, Dutcher SK, Kamiya R, Mitchell DR, Pazour GJ, Porter ME, Sale WS, Wirschell M, et al. 2011. A unified taxonomy for ciliary dyneins. *Cytoskeleton* **68**: 555–565.
- Hoops HJ, Witman GB. 1983. Outer doublet heterogeneity reveals structural polarity related to beat direction in *Chlamydomonas* flagella. *J Cell Biol* **97**: 902–908.
- Horani A, Brody SL, Ferkol TW, Shoseyov D, Wasserman MG, Ta-shma A, Wilson KS, Bayly PV, Amirav I, Cohen-Cymberknob M, et al. 2013. CCDC65 mutation causes primary ciliary dyskinesia with normal ultrastructure and hyperkinetic cilia. *PLoS ONE* **8**: e72299.
- Huang B, Piperno G, Luck DJ. 1979. Paralyzed flagella mutants of *Chlamydomonas reinhardtii*. Defective for axonemal doublet microtubule arms. *J Biol Chem* **254**: 3091–3099.
- Huang B, Ramanis Z, Luck DJ. 1982. Suppressor mutations in *Chlamydomonas* reveal a regulatory mechanism for flagellar function. *Cell* **28**: 115–124.
- Huang B, Watterson DM, Lee VD, Schibler MJ. 1988. Purification and characterization of a basal body-associated Ca²⁺-binding protein. *J Cell Biol* **107**: 121–131.

- Ichikawa M, Saito K, Yanagisawa H, Yagi T, Kamiya R, Kushida Y, Nakano K, Numata O, Toyoshima YY. 2014. Axonemal dynein light chain 1 locates at the microtubule-binding domain of the γ heavy chain. *Mol Biol Cell* **26**: 4236–4247.
- Ikedo K, Yamamoto R, Wirschell M, Yagi T, Bower R, Porter ME, Sale WS, Kamiya R. 2009. A novel ankyrin-repeat protein interacts with the regulatory proteins of inner arm dynein f (I1) of *Chlamydomonas reinhardtii*. *Cell Motil Cytoskeleton* **66**: 448–456.
- Kabututu ZP, Thayer M, Melehani JH, Hill KL. 2010. CMF70 is a subunit of the dynein regulatory complex. *J Cell Sci* **123**: 3587–3595.
- Kamiya R. 1988. Mutations at twelve independent loci result in absence of outer dynein arms in *Chlamydomonas reinhardtii*. *J Cell Biol* **107**: 2253–2258.
- Kamiya R. 1995. Exploring the function of inner and outer dynein arms with *Chlamydomonas* mutants. *Cell Motil Cytoskeleton* **32**: 98–102.
- Kamiya R, Okamoto M. 1985. A mutant of *Chlamydomonas reinhardtii* that lacks the flagellar outer dynein arm but can swim. *J Cell Sci* **74**: 181–191.
- Kamiya R, Yagi T. 2014. Functional diversity of axonemal dyneins as assessed by in vitro and in vivo motility assays of *Chlamydomonas* mutants. *Zool Sci* **31**: 633–644.
- Kamiya R, Kurimoto E, Muto E. 1991. Two types of *Chlamydomonas* flagellar mutants missing different components of inner-arm dynein. *J Cell Biol* **112**: 441–447.
- Kato T, Kagami O, Yagi T, Kamiya R. 1993. Isolation of two species of *Chlamydomonas reinhardtii* flagellar mutants, *ida5* and *ida6*, that lack a newly identified heavy chain of the inner dynein arm. *Cell Struct Funct* **18**: 371–377.
- Kato-Minoura T, Hirono M, Kamiya R. 1997. *Chlamydomonas* inner-arm dynein mutant, *ida5*, has a mutation in an actin-encoding gene. *J Cell Biol* **137**: 649–656.
- Kikkawa M. 2013. Big steps toward understanding dynein. *J Cell Biol* **202**: 15–23.
- King SM. 2010. Sensing the mechanical state of the axoneme and integration of Ca^{2+} signaling by outer arm dynein. *Cytoskeleton* **67**: 207–213.
- King SM. 2012. *Dyneins: Structure, biology and disease*. Academic, New York.
- King SM. 2013. A solid-state control system for dynein-based ciliary/flagellar motility. *J Cell Biol* **201**: 173–175.
- King SJ, Dutcher SK. 1997. Phosphoregulation of an inner dynein arm complex in *Chlamydomonas reinhardtii* is altered in phototactic mutant strains. *J Cell Biol* **136**: 177–191.
- King SM, Kamiya R. 2009. Axonemal dyneins: Assembly, structure, and force generation. In *The Chlamydomonas sourcebook: Cell motility and behavior* (ed. Witman GB), pp. 131–208. Academic, Oxford.
- King SM, Patel-King RS. 1995. The $M_r=8,000$ and 11,000 outer arm dynein light chains from *Chlamydomonas* flagella have cytoplasmic homologues. *J Biol Chem* **270**: 11445–11452.
- King SM, Patel-King RS. 2012. Functional architecture of the outer arm dynein conformational switch. *J Biol Chem* **287**: 3108–3122.
- Kotani N, Sakakibara H, Burgess SA, Kojima H, Oiwa K. 2007. Mechanical properties of inner-arm dynein-f (dynein I1) studied with in vitro motility assays. *Biophys J* **93**: 886–894.
- Koutoulis A, Pazour GJ, Wilkerson CG, Inaba K, Sheng H, Takada S, Witman GB. 1997. The *Chlamydomonas reinhardtii* ODA3 gene encodes a protein of the outer dynein arm docking complex. *J Cell Biol* **137**: 1069–1080.
- Kubo T, Yanagisawa HA, Yagi T, Hirono M, Kamiya R. 2010. Tubulin polyglutamylation regulates axonemal motility by modulating activities of inner-arm dyneins. *Curr Biol* **20**: 441–445.
- Lechtreck KF, Witman GB. 2007. *Chlamydomonas reinhardtii* hydin is a central pair protein required for flagellar motility. *J Cell Biol* **176**: 473–482.
- Lechtreck KF, Luro S, Awata J, Witman GB. 2009. HA-tagging of putative flagellar proteins in *Chlamydomonas reinhardtii* identifies a novel protein of intraflagellar transport complex B. *Cell Motil Cytoskeleton* **66**: 469–482.
- LeDizet M, Piperno G. 1995. The light chain p28 associates with a subset of inner dynein arm heavy chains in *Chlamydomonas* axonemes. *Mol Biol Cell* **6**: 697–711.
- Lin J, Tritschler D, Song K, Barber CF, Cobb JS, Porter ME, Nicastro D. 2011. Building blocks of the nexin-dynein regulatory complex in *Chlamydomonas* flagella. *J Biol Chem* **286**: 29175–29191.
- Lin J, Heuser T, Carbajal-Gonzalez BI, Song K, Nicastro D. 2012. The structural heterogeneity of radial spokes in cilia and flagella is conserved. *Cytoskeleton* **69**: 88–100.
- Lin J, Okada K, Raytchev M, Smith MC, Nicastro D. 2014a. Structural mechanism of the dynein power stroke. *Nat Cell Biol* **16**: 479–485.
- Lin J, Yin W, Smith MC, Song K, Leigh MW, Zariwala MA, Knowles MR, Ostrowski LE, Nicastro D. 2014b. Cryo-electron tomography reveals ciliary defects underlying human RSPH1 primary ciliary dyskinesia. *Nat Commun* **5**: 5727.
- Lin H, Zhang Z, Guo S, Chen F, Kessler JM, Wang YM, Dutcher SK. 2015. A NIMA-related kinase suppresses the flagellar instability associated with the loss of multiple axonemal structures. *PLoS Genet* **11**: e1005508.
- Lindemann CB, Mitchell DR. 2007. Evidence for axonemal distortion during the flagellar beat of *Chlamydomonas*. *Cell Motil Cytoskeleton* **64**: 580–589.
- Lindemann CB, Lesich KA. 2010. Flagellar and ciliary beating: The proven and the possible. *J Cell Sci* **123**: 519–528.
- Mastroratte DN, O'Toole ET, McDonald KL, McIntosh JR, Porter ME. 1992. Arrangement of inner dynein arms in wild-type and mutant flagella of *Chlamydomonas*. *J Cell Biol* **118**: 1145–1162.
- Merveille AC, Davis EE, Becker-Heck A, Legendre M, Amirav I, Bataille G, Belmont J, Beydon N, Billen F, Clement A, et al. 2011. CCDC39 is required for assembly of inner dynein arms and the dynein regulatory complex and for normal ciliary motility in humans and dogs. *Nat Genet* **43**: 72–78.
- Mitchell DR, Brown KS. 1994. Sequence analysis of the *Chlamydomonas* α and β dynein heavy chain genes. *J Cell Sci* **107** (Pt 3): 635–644.
- Mitchell DR, Brown KS. 1997. Sequence analysis of the *Chlamydomonas reinhardtii* flagellar alpha dynein gene. *Cell Motil Cytoskeleton* **37**: 120–126.
- Mitchell DR, Kang Y. 1991. Identification of *oda6* as a *Chlamydomonas* dynein mutant by rescue with the wild-type gene. *J Cell Biol* **113**: 835–842.
- Mitchell DR, Nakatsugawa M. 2004. Bend propagation drives central pair rotation in *Chlamydomonas reinhardtii* flagella. *J Cell Biol* **166**: 709–715.
- Mitchell DR, Rosenbaum JL. 1985. A motile *Chlamydomonas* flagellar mutant that lacks outer dynein arms. *J Cell Biol* **100**: 1228–1234.
- Mitchison HM, Schmidts M, Loges NT, Freshour J, Dritsoula A, Hirst RA, O'Callaghan C, Blau H, Al Dabbagh M, Olbrich H, et al. 2012. Mutations in axonemal dynein assembly factor DNAAF3 cause primary ciliary dyskinesia. *Nat Genet* **44**: 381–389.
- Morita Y, Shingyoji C. 2004. Effects of imposed bending on microtubule sliding in sperm flagella. *Curr Biol* **14**: 2113–2118.
- Movassagh T, Bui KH, Sakakibara H, Oiwa K, Ishikawa T. 2010. Nucleotide-induced global conformational changes of flagellar dynein arms revealed by in situ analysis. *Nat Struct Mol Biol* **17**: 761–767.
- Myster SH, Knott JA, O'Toole E, Porter ME. 1997. The *Chlamydomonas* *Dhc1* gene encodes a dynein heavy chain subunit required for assembly of the I1 inner arm complex. *Mol Biol Cell* **8**: 607–620.
- Myster SH, Knott JA, Wysocki KM, O'Toole E, Porter ME. 1999. Domains in the α dynein heavy chain required for inner arm assembly and flagellar motility in *Chlamydomonas*. *J Cell Biol* **146**: 801–818.
- Nicastro D. 2009. Cryo-electron microscope tomography to study axonemal organization. *Methods Cell Biol* **91**: 1–39.
- Nicastro D, Schwartz C, Pierson J, Gaudette R, Porter ME, McIntosh JR. 2006. The molecular architecture of axonemes revealed by cryoelectron tomography. *Science* **313**: 944–948.

- Oda T, Kikkawa M. 2013. Novel structural labeling method using cryo-electron tomography and biotin-streptavidin system. *J Struct Biol* **183**: 305–311.
- Oda T, Yagi T, Yanagisawa H, Kikkawa M. 2013. Identification of the outer-inner dynein linker as a hub controller for axonemal dynein activities. *Curr Biol* **23**: 656–664.
- Oda T, Yanagisawa H, Kamiya R, Kikkawa M. 2014a. A molecular ruler determines the repeat length in eukaryotic cilia and flagella. *Science* **346**: 857–860.
- Oda T, Yanagisawa H, Yagi T, Kikkawa M. 2014b. Mechanosignaling between central apparatus and radial spokes controls axonemal dynein activity. *J Cell Biol* **204**: 807–819.
- Oda T, Yanagisawa H, Kikkawa M. 2015. Detailed structural and biochemical characterization of the nexin-dynein regulatory complex. *Mol Biol Cell* **26**: 294–304.
- Olbrich H, Cremers C, Loges NT, Werner C, Nielsen KG, Marthin JK, Philippen M, Wallmeier J, Pennekamp P, Menchen T, et al. 2015. Loss-of-function GAS8 mutations cause primary ciliary dyskinesia and disrupt the nexin-dynein regulatory complex. *Am J Hum Genet* **97**: 546–554.
- Omran H, Kobayashi D, Olbrich H, Tsukahara T, Loges N, Hagiwara H, Zhang Q, Leblond G, O'Toole E, Hara C, et al. 2008. Ktu/PF13 is required for cytoplasmic pre-assembly of axonemal dyneins. *Nature* **456**: 611–616.
- O'Toole ET, Giddings TH Jr., Porter ME, Ostrowski LE. 2012. Computer-assisted image analysis of human cilia and *Chlamydomonas* flagella reveals both similarities and differences in axoneme structure. *Cytoskeleton* **69**: 577–590.
- Owa M, Furuta A, Usukura J, Arisaka F, King SM, Witman GB, Kamiya R, Wakabayashi K. 2014. Cooperative binding of the outer arm-docking complex underlies the regular arrangement of outer arm dynein in the axoneme. *Proc Natl Acad Sci* **111**: 9461–9466.
- Patel-King RS, King SM. 2009. An outer arm dynein light chain acts in a conformational switch for flagellar motility. *J Cell Biol* **186**: 283–295.
- Patel-King RS, Benashski SE, Harrison A, King SM. 1997. A *Chlamydomonas* homologue of the putative murine t complex distorter Tctex-2 is an outer arm dynein light chain. *J Cell Biol* **137**: 1081–1090.
- Patel-King RS, Gorbatyuk O, Takebe S, King SM. 2004. Flagellar radial spokes contain a Ca²⁺-stimulated nucleoside diphosphate kinase. *Mol Biol Cell* **15**: 3891–3902.
- Pazour GJ, Koutoulis A, Benashski SE, Dickert BL, Sheng H, Patel-King RS, King SM, Witman GB. 1999. LC2, the *Chlamydomonas* homologue of the t complex-encoded protein Tctex2, is essential for outer dynein arm assembly. *Mol Biol Cell* **10**: 3507–3520.
- Perrone CA, Yang P, O'Toole E, Sale WS, Porter ME. 1998. The *Chlamydomonas* IDA7 locus encodes a 140-kDa dynein intermediate chain required to assemble the I1 inner arm complex. *Mol Biol Cell* **9**: 3351–3365.
- Perrone CA, Myster SH, Bower R, O'Toole ET, Porter ME. 2000. Insights into the structural organization of the I1 inner arm dynein from a domain analysis of the I β dynein heavy chain. *Mol Biol Cell* **11**: 2297–2313.
- Pigino G, Bui KH, Maheshwari A, Lupetti P, Diener D, Ishikawa T. 2011. Cryoelectron tomography of radial spokes in cilia and flagella. *J Cell Biol* **195**: 673–687.
- Pigino G, Maheshwari A, Bui KH, Shingyoji C, Kamimura S, Ishikawa T. 2012. Comparative structural analysis of eukaryotic flagella and cilia from *Chlamydomonas*, *Tetrahymena*, and sea urchins. *J Struct Biol* **178**: 199–206.
- Piperno G, Ramanis Z, Smith EF, Sale WS. 1990. Three distinct inner dynein arms in *Chlamydomonas* flagella: Molecular composition and location in the axoneme. *J Cell Biol* **110**: 379–389.
- Piperno G, Mead K, Shestak W. 1992. The inner dynein arms I2 interact with a “dynein regulatory complex” in *Chlamydomonas* flagella. *J Cell Biol* **118**: 1455–1463.
- Piperno G, Mead K, LeDizet M, Moscatelli A. 1994. Mutations in the “dynein regulatory complex” alter the ATP-insensitive binding sites for inner arm dyneins in *Chlamydomonas* axonemes. *J Cell Biol* **125**: 1109–1117.
- Porter ME. 2012. Flagellar motility and the dynein regulatory complex. In *Dyneins: Structure, biology and disease* (ed. King SM), pp. 337–365. Academic, New York.
- Porter ME, Sale WS. 2000. The 9 + 2 axoneme anchors multiple inner arm dyneins and a network of kinases and phosphatases that control motility. *J Cell Biol* **151**: F37–F42.
- Porter ME, Power J, Dutcher SK. 1992. Extragenic suppressors of paralyzed flagellar mutations in *Chlamydomonas reinhardtii* identify loci that alter the inner dynein arms. *J Cell Biol* **118**: 1163–1176.
- Porter ME, Knott JA, Gardner LC, Mitchell DR, Dutcher SK. 1994. Mutations in the SUP-PF-1 locus of *Chlamydomonas reinhardtii* identify a regulatory domain in the β -dynein heavy chain. *J Cell Biol* **126**: 1495–1507.
- Porter ME, Knott JA, Myster SH, Farlow SJ. 1996. The dynein gene family in *Chlamydomonas reinhardtii*. *Genetics* **144**: 569–585.
- Porter ME, Bower R, Knott JA, Byrd P, Dentler W. 1999. Cytoplasmic dynein heavy chain 1b is required for flagellar assembly in *Chlamydomonas*. *Mol Biol Cell* **10**: 693–712.
- Ralston KS, Hill KL. 2006. Trypanin, a component of the flagellar dynein regulatory complex, is essential in bloodstream form African trypanosomes. *PLoS Pathog* **2**: e101.
- Rupp G, Porter ME. 2003. A subunit of the dynein regulatory complex in *Chlamydomonas* is a homologue of a growth arrest-specific gene product. *J Cell Biol* **162**: 47–57.
- Rupp G, O'Toole E, Gardner LC, Mitchell BF, Porter ME. 1996. The sup-pf-2 mutations of *Chlamydomonas* alter the activity of the outer dynein arms by modification of the γ -dynein heavy chain. *J Cell Biol* **135**: 1853–1865.
- Sakato M, Sakakibara H, King SM. 2007. *Chlamydomonas* outer arm dynein alters conformation in response to Ca²⁺. *Mol Biol Cell* **18**: 3620–3634.
- Sale WS, Satir P. 1977. Direction of active sliding of microtubules in *Tetrahymena* cilia. *Proc Natl Acad Sci* **74**: 2045–2049.
- Sanders MA, Salisbury JL. 1989. Centrin-mediated microtubule severing during flagellar excision in *Chlamydomonas reinhardtii*. *J Cell Biol* **108**: 1751–1760.
- Satir P. 1968. Studies on cilia. 3. Further studies on the cilium tip and a “sliding filament” model of ciliary motility. *J Cell Biol* **39**: 77–94.
- Satir P, Matsuoka T. 1989. Splitting the ciliary axoneme: Implications for a “switch-point” model of dynein arm activity in ciliary motion. *Cell Motil Cytoskeleton* **14**: 345–358.
- Satir P, Heuser T, Sale WS. 2014. A structural basis for how motile cilia beat. *Bioscience* **64**: 1073–1083.
- Shingyoji C, Murakami A, Takahashi K. 1977. Local reactivation of Triton-extracted flagella by iontophoretic application of ATP. *Nature* **265**: 269–270.
- Sivadas P, Dienes JM, St Maurice M, Meek WD, Yang P. 2012. A flagellar A-kinase anchoring protein with two amphipathic helices forms a structural scaffold in the radial spoke complex. *J Cell Biol* **199**: 639–651.
- Smith EF. 2002. Regulation of flagellar dynein by calcium and a role for an axonemal calmodulin and calmodulin-dependent kinase. *Mol Biol Cell* **13**: 3303–3313.
- Smith EF. 2007. Hydin seek: Finding a function in ciliary motility. *J Cell Biol* **176**: 403–404.
- Smith EF, Sale WS. 1992a. Regulation of dynein-driven microtubule sliding by the radial spokes in flagella. *Science* **257**: 1557–1559.
- Smith EF, Sale WS. 1992b. Structural and functional reconstitution of inner dynein arms in *Chlamydomonas* flagellar axonemes. *J Cell Biol* **117**: 573–581.
- Smith EF, Yang P. 2004. The radial spokes and central apparatus: Mechano-chemical transducers that regulate flagellar motility. *Cell Motil Cytoskeleton* **57**: 8–17.
- Song K, Awata J, Tritschler D, Bower R, Witman GB, Porter ME, Nicastro D. 2015. In situ localization of N and C termini of subunits of the

- flagellar nexin-dynein regulatory complex (N-DRC) using SNAP tag and cryo-electron tomography. *J Biol Chem* **290**: 5341–5353.
- Stephens RE. 1970. Isolation of nexin—The linkage protein responsible for maintenance of nine-fold configuration of flagellar axonemes. *Biol Bull* **139**: 438.
- Summers KE, Gibbons IR. 1971. Adenosine triphosphate-induced sliding of tubules in trypsin-treated flagella of sea-urchin sperm. *Proc Natl Acad Sci* **68**: 3092–3096.
- Takada S, Kamiya R. 1994. Functional reconstitution of *Chlamydomonas* outer dynein arms from α - β and γ subunits: Requirement of a third factor. *J Cell Biol* **126**: 737–745.
- Takada S, Wilkerson CG, Wakabayashi K, Kamiya R, Witman GB. 2002. The outer dynein arm-docking complex: Composition and characterization of a subunit (oda1) necessary for outer arm assembly. *Mol Biol Cell* **13**: 1015–1029.
- Toba S, Fox LA, Sakakibara H, Porter ME, Oiwa K, Sale WS. 2011. Distinct roles of 1α and 1β heavy chains of the inner arm dynein I1 of *Chlamydomonas* flagella. *Mol Biol Cell* **22**: 342–353.
- VanderWaal KE, Yamamoto R, Wakabayashi K, Fox L, Kamiya R, Dutcher SK, Bayly PV, Sale WS, Porter ME. 2011. bop5 Mutations reveal new roles for the IC138 phosphoprotein in the regulation of flagellar motility and asymmetric waveforms. *Mol Biol Cell* **22**: 2862–2874.
- Vasudevan KK, Song K, Alford LM, Sale WS, Dymek EE, Smith EF, Hennessey T, Joachimiak E, Urbanska P, Wloga D, et al. 2015. FAP206 is a microtubule-docking adapter for ciliary radial spoke 2 and dynein c. *Mol Biol Cell* **26**: 696–710.
- Viswanadha R, Hunter EL, Yamamoto R, Wirschell M, Alford LM, Dutcher SK, Sale WS. 2014. The ciliary inner dynein arm, I1 dynein, is assembled in the cytoplasm and transported by IFT before axonemal docking. *Cytoskeleton* **71**: 573–586.
- Wakabayashi K, King SM. 2006. Modulation of *Chlamydomonas reinhardtii* flagellar motility by redox poise. *J Cell Biol* **173**: 743–754.
- Wargo MJ, Smith EF. 2003. Asymmetry of the central apparatus defines the location of active microtubule sliding in *Chlamydomonas* flagella. *Proc Natl Acad Sci* **100**: 137–142.
- Warner FD. 1976. Ciliary inter-microtubule bridges. *J Cell Sci* **20**: 101–114.
- Warner FD. 1983. Organization of interdoublet links in *Tetrahymena* cilia. *Cell Motil Cytoskel* **3**: 321–332.
- Warner FD, Satir P. 1974. The structural basis of ciliary bend formation. Radial spoke positional changes accompanying microtubule sliding. *J Cell Biol* **63**: 35–63.
- Wickstead B, Gull K. 2007. Dyneins across eukaryotes: A comparative genomic analysis. *Traffic* **8**: 1708–1721.
- Wilkerson CG, King SM, Witman GB. 1994. Molecular analysis of the γ heavy chain of *Chlamydomonas* flagellar outer-arm dynein. *J Cell Sci* **107** (Pt 3): 497–506.
- Wilkerson CG, King SM, Koutoulis A, Pazour GJ, Witman GB. 1995. The 78,000- M_r intermediate chain of *Chlamydomonas* outer arm dynein is a WD-repeat protein required for arm assembly. *J Cell Biol* **129**: 169–178.
- Williams BD, Velleca MA, Curry AM, Rosenbaum JL. 1989. Molecular cloning and sequence analysis of the *Chlamydomonas* gene coding for radial spoke protein 3: Flagellar mutation *pf-14* is an ochre allele. *J Cell Biol* **109**: 235–245.
- Wirschell M, Pazour G, Yoda A, Hirono M, Kamiya R, Witman GB. 2004. Oda5p, a novel axonemal protein required for assembly of the outer dynein arm and an associated adenylate kinase. *Mol Biol Cell* **15**: 2729–2741.
- Wirschell M, Hendrickson T, Sale WS. 2007. Keeping an eye on I1: I1 dynein as a model for flagellar dynein assembly and regulation. *Cell Motil Cytoskeleton* **64**: 569–579.
- Wirschell M, Yang C, Yang P, Fox L, Yanagisawa HA, Kamiya R, Witman GB, Porter ME, Sale WS. 2009. IC97 Is a novel intermediate chain of I1 dynein that interacts with tubulin and regulates interdoublet sliding. *Mol Biol Cell* **20**: 3044–3054.
- Wirschell M, Olbrich H, Werner C, Tritschler D, Bower R, Sale WS, Loges NT, Pennekamp P, Lindberg S, Stenram U, et al. 2013. The nexin-dynein regulatory complex subunit DRC1 is essential for motile cilia function in algae and humans. *Nat Genet* **45**: 262–268.
- Witman GB, Plummer J, Sander G. 1978. *Chlamydomonas* flagellar mutants lacking radial spokes and central tubules. Structure, composition, and function of specific axonemal components. *J Cell Biol* **76**: 729–747.
- Woolley DM. 1997. Studies on the eel sperm flagellum. I. The structure of the inner dynein arm complex. *J Cell Sci* **110**: 85–94.
- Wu H, Maciejewski MW, Takebe S, King SM. 2005. Solution structure of the Tctex1 dimer reveals a mechanism for dynein-cargo interactions. *Structure* **13**: 213–223.
- Yagi T, Minoura I, Fujiwara A, Saito R, Yasunaga T, Hirono M, Kamiya R. 2005. An axonemal dynein particularly important for flagellar movement at high viscosity. Implications from a new *Chlamydomonas* mutant deficient in the dynein heavy chain gene *DHC9*. *J Biol Chem* **280**: 41412–41420.
- Yagi T, Uematsu K, Liu Z, Kamiya R. 2009. Identification of dyneins that localize exclusively to the proximal portion of *Chlamydomonas* flagella. *J Cell Sci* **122**: 1306–1314.
- Yamamoto R, Yanagisawa HA, Yagi T, Kamiya R. 2006. A novel subunit of axonemal dynein conserved among lower and higher eukaryotes. *FEBS Lett* **580**: 6357–6360.
- Yamamoto R, Yanagisawa HA, Yagi T, Kamiya R. 2008. Novel 44-kilodalton subunit of axonemal dynein conserved from *Chlamydomonas* to mammals. *Eukaryot Cell* **7**: 154–161.
- Yamamoto R, Hirono M, Kamiya R. 2010. Discrete PIH proteins function in the cytoplasmic preassembly of different subsets of axonemal dyneins. *J Cell Biol* **190**: 65–71.
- Yamamoto R, Song K, Yanagisawa HA, Fox L, Yagi T, Wirschell M, Hirono M, Kamiya R, Nicastro D, Sale WS. 2013. The MIA complex is a conserved and novel dynein regulator essential for normal ciliary motility. *J Cell Biol* **201**: 263–278.
- Yanagisawa HA, Kamiya R. 2001. Association between actin and light chains in *Chlamydomonas* flagellar inner-arm dyneins. *Biochem Biophys Res Commun* **288**: 443–447.
- Yanagisawa HA, Kamiya R. 2004. A tektin homologue is decreased in *Chlamydomonas* mutants lacking an axonemal inner-arm dynein. *Mol Biol Cell* **15**: 2105–2115.
- Yang P, Sale WS. 1998. The M_r 140,000 intermediate chain of *Chlamydomonas* flagellar inner arm dynein is a WD-repeat protein implicated in dynein arm anchoring. *Mol Biol Cell* **9**: 3335–3349.
- Yang P, Sale WS. 2000. Casein kinase I is anchored on axonemal doublet microtubules and regulates flagellar dynein phosphorylation and activity. *J Biol Chem* **275**: 18905–18912.
- Yang P, Diener DR, Rosenbaum JL, Sale WS. 2001. Localization of calmodulin and dynein light chain LC8 in flagellar radial spokes. *J Cell Biol* **153**: 1315–1326.
- Yang P, Diener DR, Yang C, Kohno T, Pazour GJ, Dienes JM, Agrin NS, King SM, Sale WS, Kamiya R, et al. 2006. Radial spoke proteins of *Chlamydomonas* flagella. *J Cell Sci* **119**: 1165–1174.
- Yang P, Yang C, Wirschell M, Davis S. 2009. Novel LC8 mutations have disparate effects on the assembly and stability of flagellar complexes. *J Biol Chem* **284**: 31412–31421.
- Yang Y, Cochran DA, Gargano MD, King I, Samhat NK, Burger BP, Sabourin KR, Hou Y, Awata J, Parry DA, et al. 2011. Regulation of flagellar motility by the conserved flagellar protein CG34110/Ccdc135/FAP50. *Mol Biol Cell* **22**: 976–987.
- Zhang D, Aravind L. 2012. Novel transglutaminase-like peptidase and C2 domains elucidate the structure, biogenesis and evolution of the ciliary compartment. *Cell Cycle* **11**: 3861–3875.